The equation of state of compact stars in the gravitational wave era

David E. Álvarez Castillo
Joint Institute for Nuclear Research
Dubna, Russia

Zimányi School 2019
Budapest, Hungary
December 5, 2019

Outline

- A brief introduction to the neutron star matter equation of state and its location within the QCD phase diagram.
- The compact star mass twins hypothesis.
- Astrophysics measurements of compact stars: multi-messenger astronomy & the GW170817 event.
- Astrophysical implications and perspectives.

Double Neutron Stars and Millisecond Pulsars

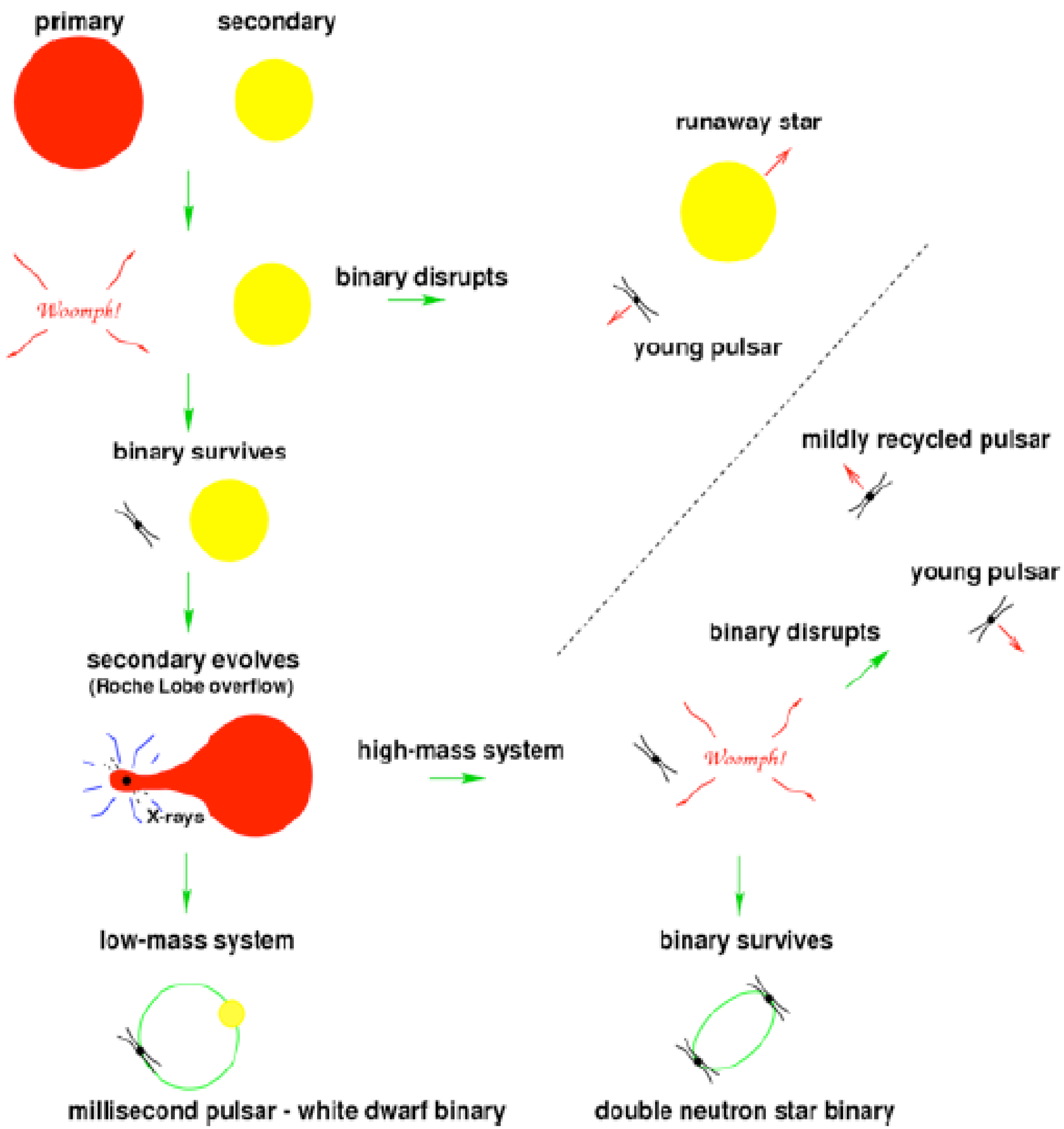

Pulse shapes and el.-magn. spectrum

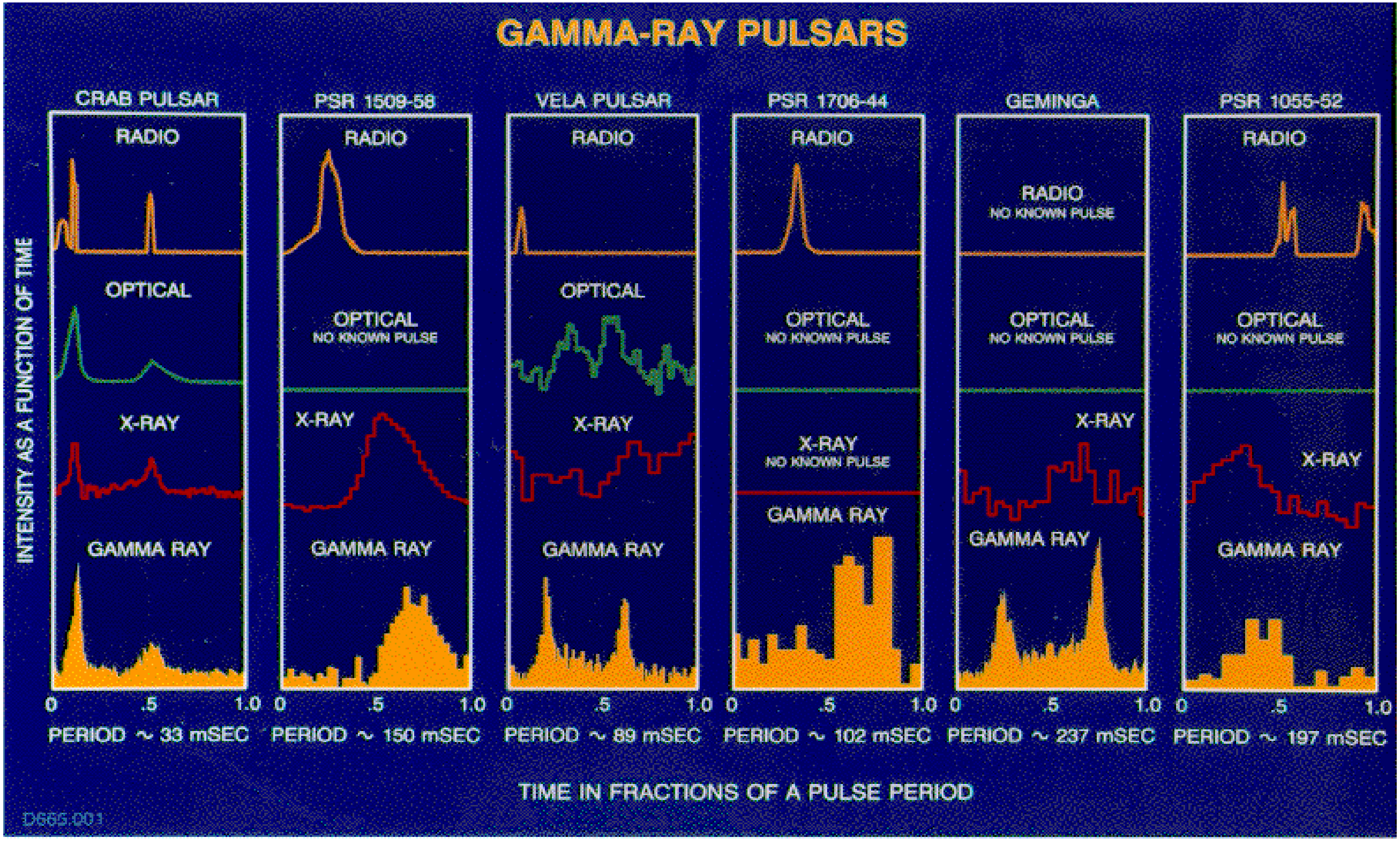

Statistics of Pulsars

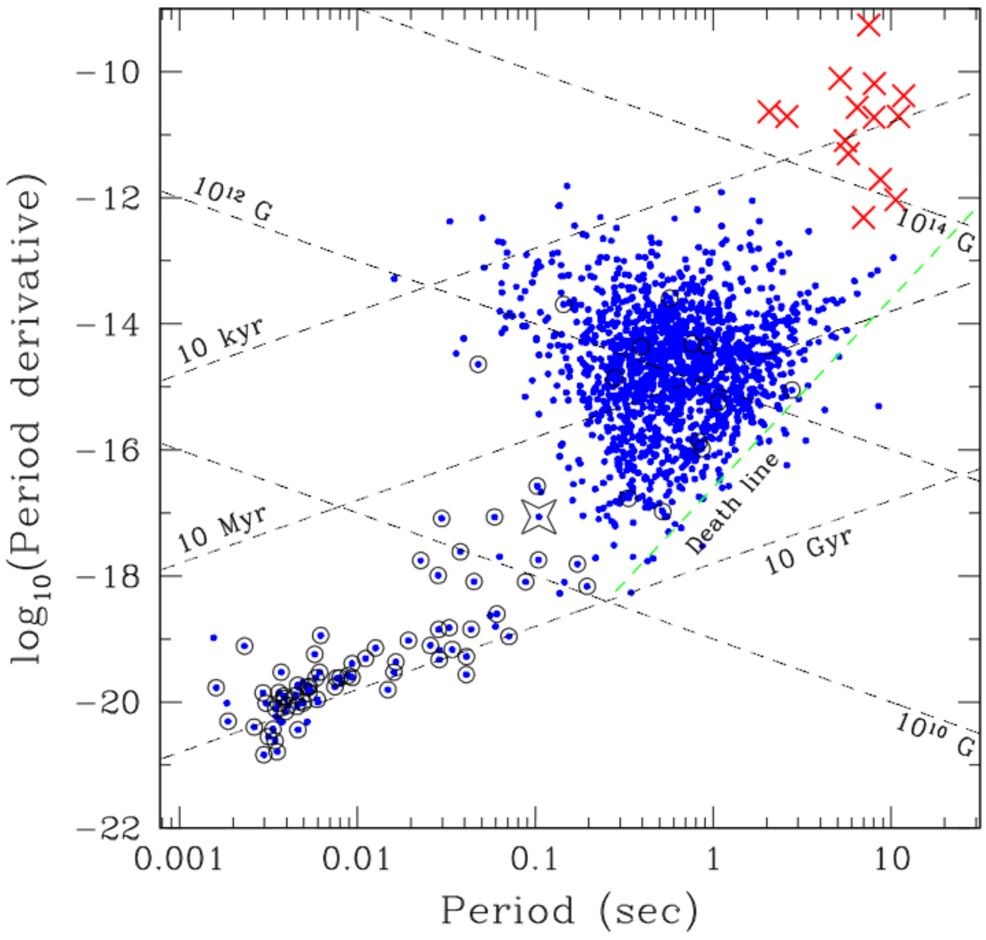

Magnetars:
$B > 10^{15}$ Gauss

Young pulsars:
$P < 1$ sec
$B \sim 10^{12}$ Gauss

Recycled (old) Pulsars:
$P \sim$ few milliseconds
$B \sim 10^{8}$ Gauss

Superdense objects – what is inside?

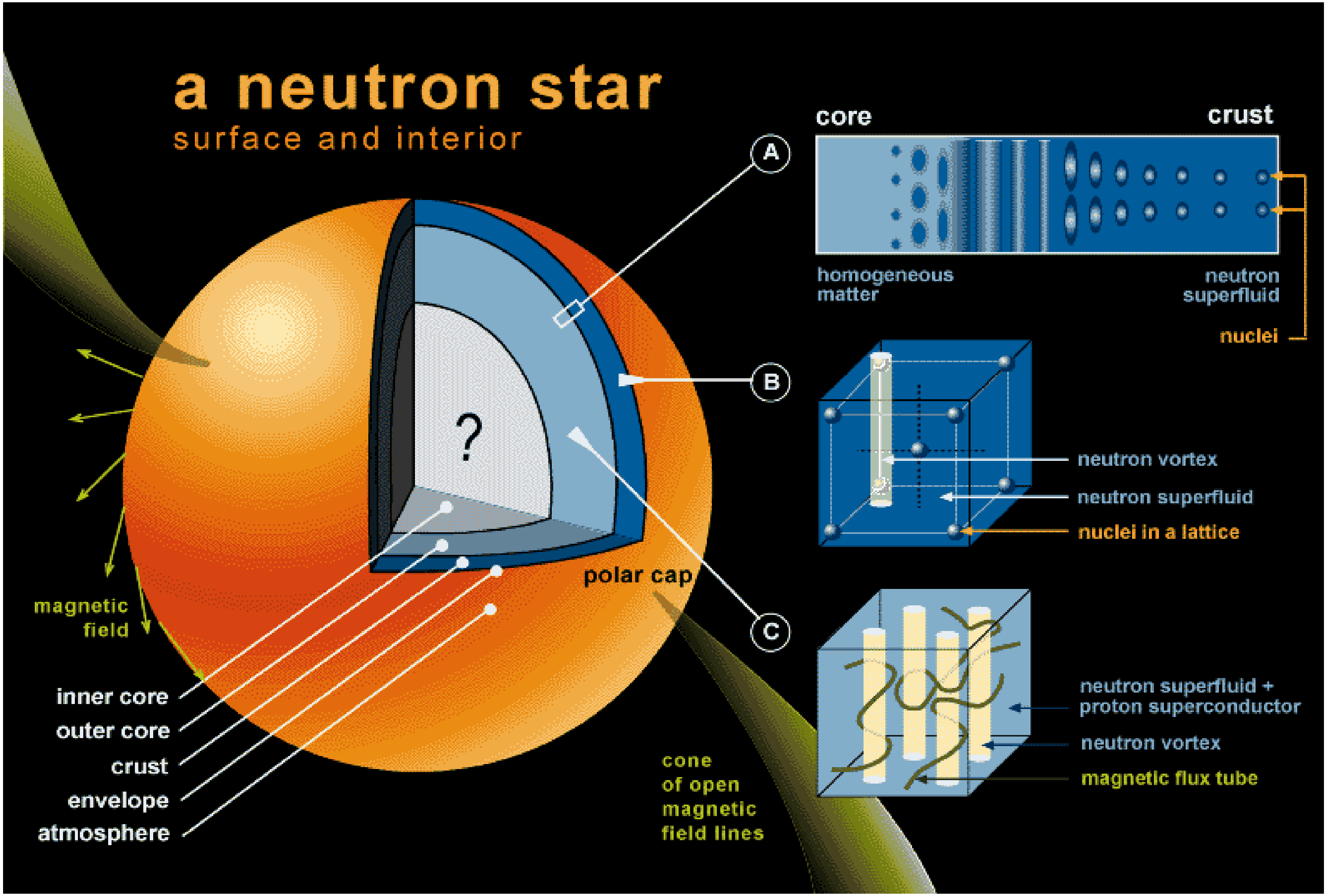

Superdense objects – what is inside?

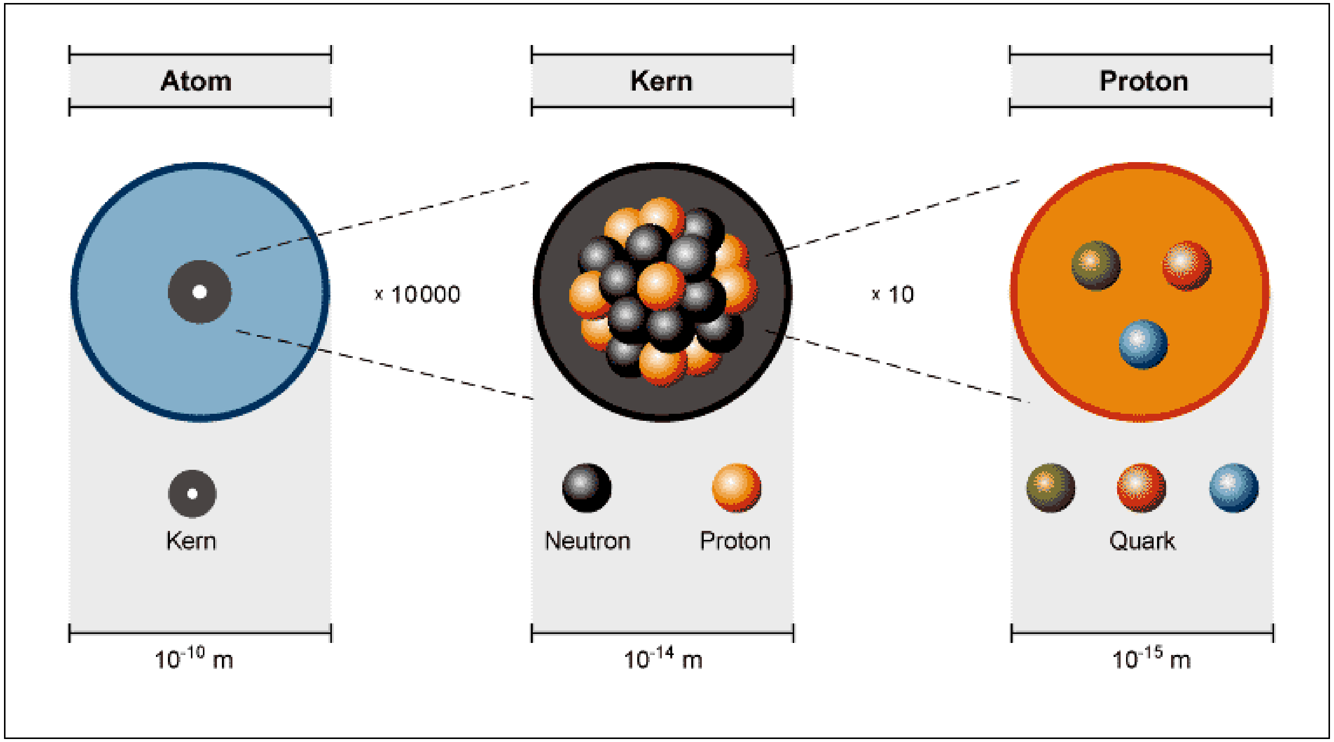

Nucleus, A nucleons: R_A=1.2 10^{-13} cm $A^{1/3}$; ρ_0=A1.67 10^{-24} g/(4π/3 $R_A^{\,3}$)= 2.3 10^{14} g/cm^3

Neutron star: R= 10 km; ρ= 2 Mo/(4π/3 R^3) = 4 10^{33} g/(4 10^{18} cm^3)= 10^{15} g/cm^3 = 4 ρ_0

Nuclear Matter

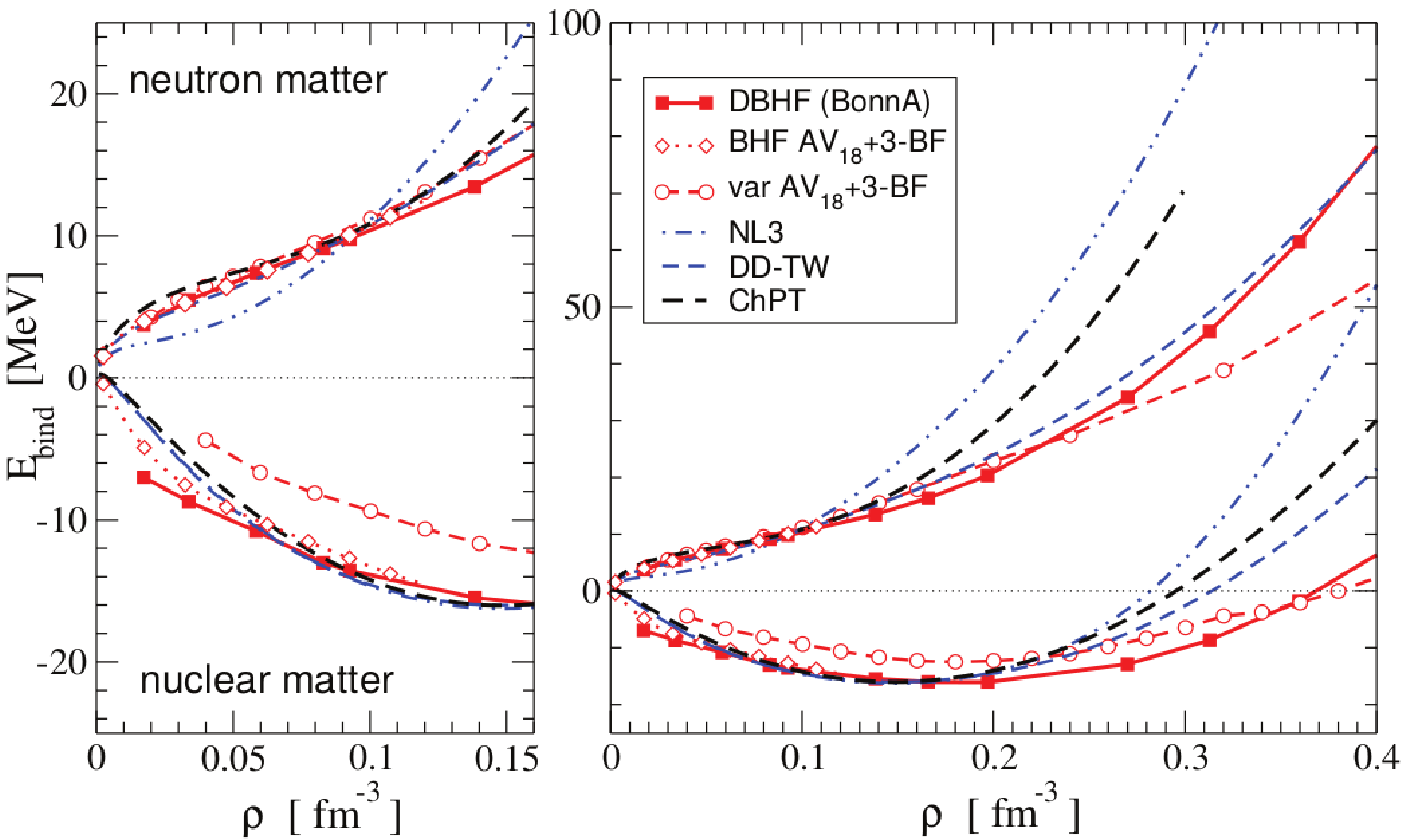

C. Fuchs, H.H. Wolter, EPJA 30(2006)5

Neutron Star Equation of State

The energy per nucleon in neutron star core matter is given by:

$$\begin{aligned} E_{\text{tot}}(n,\{x_i\}) &= E_{\text{b}}(n,x_p)+E_{\text{lep}}(n,x_e,x_\mu)\ , \\ E_{\text{b}}(n,x_p) &= E_0(n)+S(n,x_p) \\ E_{\text{lep}}(n,x_e,x_\mu) &= E_e(n,x_e)+E_\mu(n,x_\mu)\ , \end{aligned}$$

where $n = n_p + n_n$ is the total baryon density and $x_i = n_i/n$, $i = p, e, \mu$ are the fractions of protons, electrons and muons, respectively. The baryonic part is very well described by the parabolic approximation w.r.t. the asymmetry

$$\alpha = \frac{n_n - n_p}{n_n + n_p} = 1 - 2x_p,$$

resulting in $S(n, x_p) = (1 - 2x_p)^2 E_s(n)$. The leptonic contribution is a sum of the Fermi gas expressions for the contributing leptons $l = e, \mu$

$$E_l(n,x_l) = \frac{1}{n}\frac{p_{F,l}^4}{4\pi^2}\left[\sqrt{1+z_l^2}\left(1+\frac{z_l^2}{2}\right) - \frac{z_l^4}{2}\text{Arsinh}\left(\frac{1}{z_l}\right)\right]\ ,$$

where $z_l = m_l/p_{F,l}$. For massless leptons ($z_l \to 0$), this expression goes over to

$$E_l(n,x_l)\big|_{m_l=0} = \frac{1}{n}\frac{p_{F,l}^4}{4\pi^2} = \frac{3}{4}\left(3\pi^2 n\right)^{1/3} x_l^{4/3}\ .$$

Charge neutrality and β-equillibrium

Under neutron star conditions charge neutrality holds,

$$x_p = x_e + x_\mu \ .$$

The $\beta-$ equilibrium with respect to the weak interaction processes $n \to p + e^- + \bar{\nu}_e$ and $p + e^- \to n + \nu_e$ (and similar for muons), for cold neutron stars (temperature T below the neutrino opacity criterion $T < T_\nu \sim 1$ MeV) implies

$$\mu_n - \mu_p = \mu_e = \mu_\mu \ .$$

The chemical potentials are defined as

$$\mu_i = \frac{\partial \varepsilon_i}{\partial n_i} = \frac{\partial}{\partial x_i} E_i(n, \{x_j\}) \ , \quad i, j = n, p, e, \mu \ ,$$

where $\varepsilon_i = n \ E_i(n, \{x_j\})$ is the partial energy density of species i in the system. From the above equations:

$$\mu_e = 4(1 - 2x) E_s(n) \ .$$

Since electrons in neutron star interiors are ultrarelativistic,

$$\mu_e = \sqrt{p_{F,e}^2 + m_e^2} \approx p_{F,e}, \text{ and } p_{F,e} = (3\pi^2 n_e)^{1/3} = (3\pi^2 n)^{1/3} (x - x_\mu)^{1/3} \ ,$$

$$\frac{x - x_\mu}{(1 - 2x)^3} = \frac{64 E_s^3(n)}{3\pi^2 n} \ , \qquad (x - x_\mu)^{2/3} - x_\mu^{2/3} = \frac{m_\mu^2}{(3\pi^2 n)^{2/3}} \ .$$

The total pressure is then given as $P(n) = n^2 \left(\frac{\partial E_{\mathrm{tot}}}{\partial n} \right) \ .$

Compact Star Sequences

(M-R ⇔ EoS)

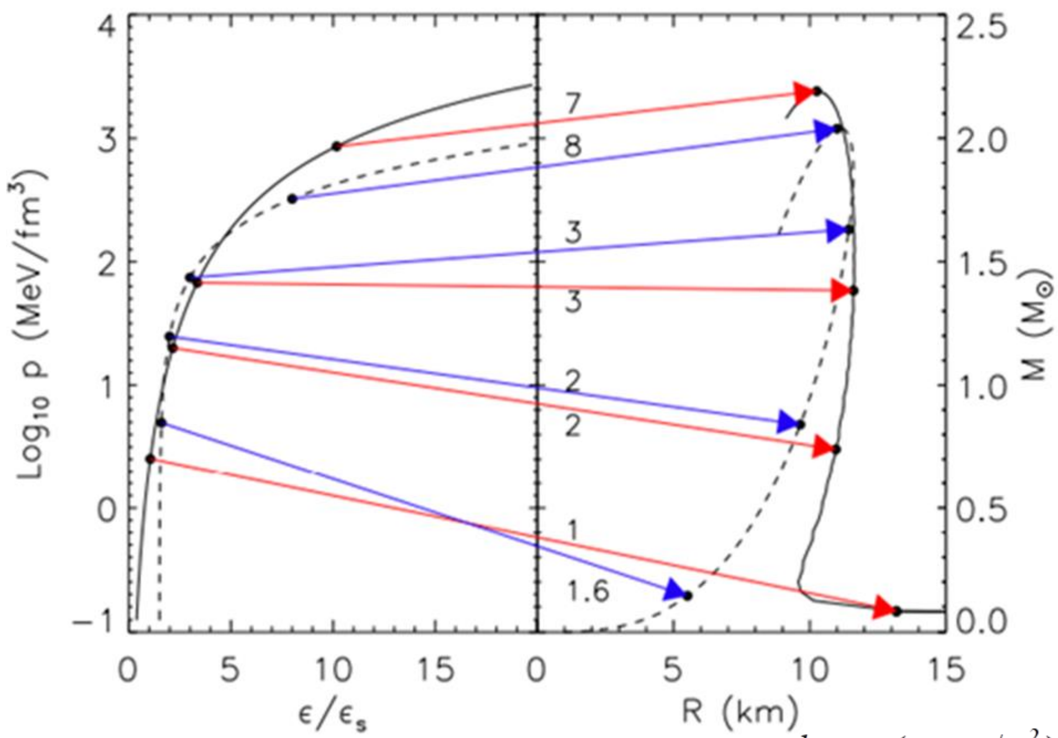

Lattimer,
Annu. Rev. Nucl. Part. Sci.
62, 485 (2012)
arXiv: 1305.3510

- TOV Equations

$$\frac{dp}{dr} = -\frac{(\varepsilon + p/c^2)G(m + 4\pi r^3 p/c^2)}{r^2(1 - 2Gm/rc^2)}$$

$$\frac{dm}{dr} = 4\pi r^2 \varepsilon$$

- Equation of State (EoS)

$$p(\varepsilon)$$

Flow Constraint

Klaehn et al. PhysRev C74 (2006)

P. Danielewicz, R. Lacey and W.G. Lynch, Science 298, 1592 (2002)

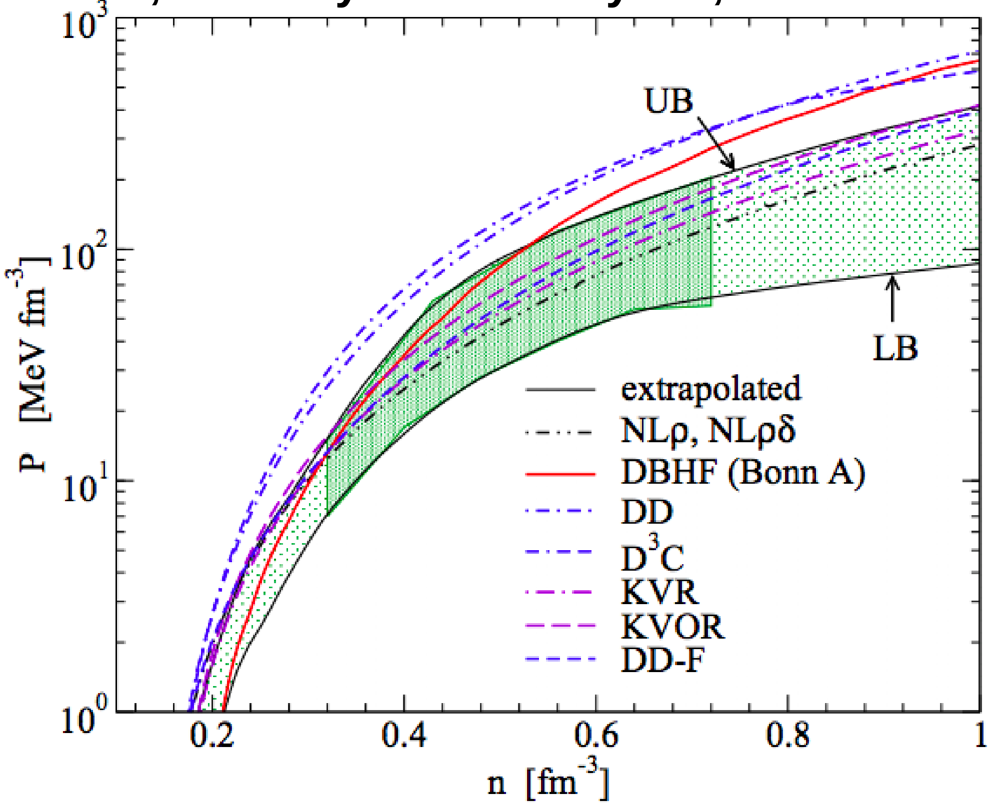

FIG. 6: Pressure region consistent with experimental flow data in SNM (dark shaded region). The light shaded region extrapolates this region to higher densities within an upper (UB) and lower border (LB).

EoS Stiffness

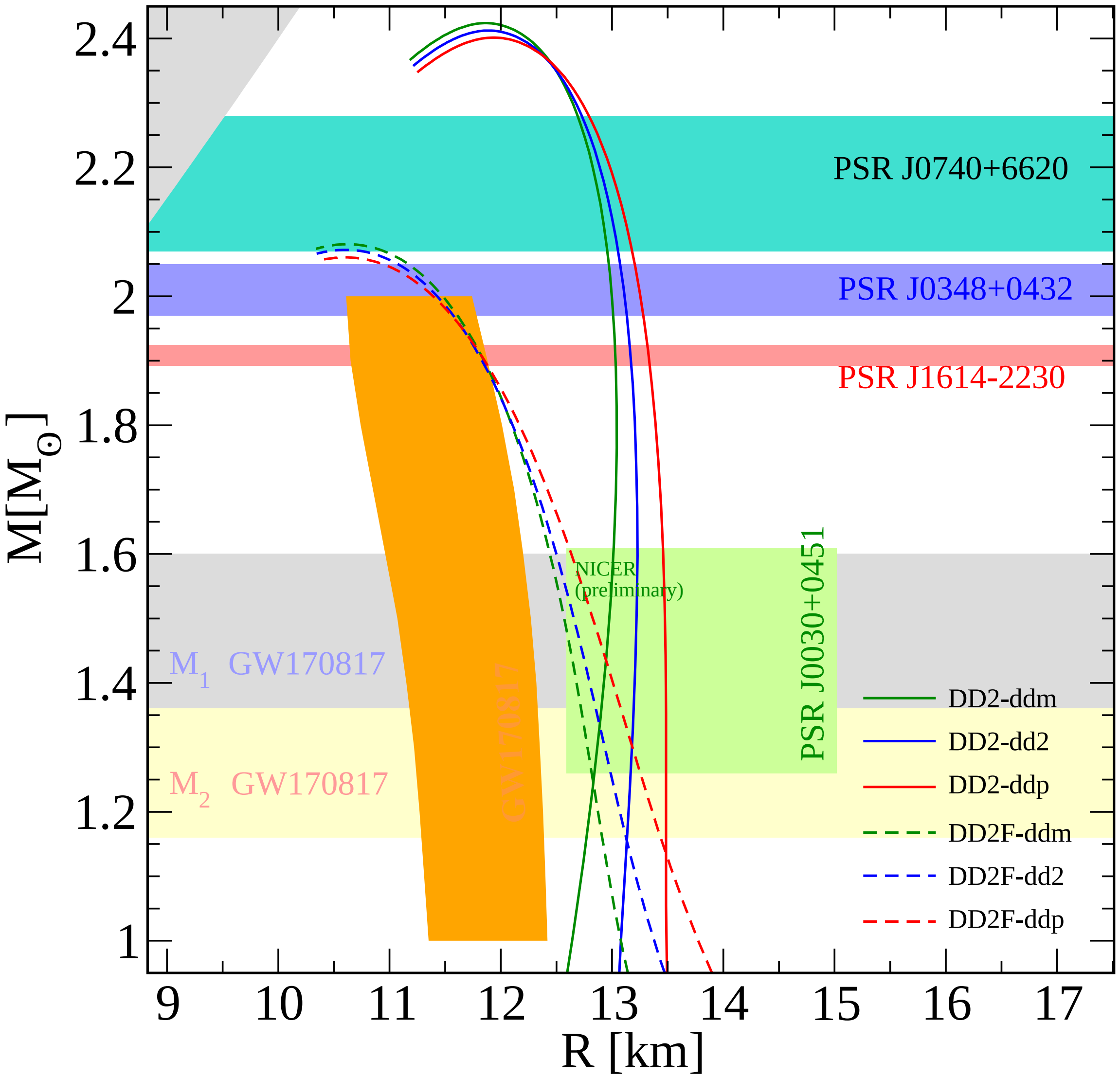

SPACE + SCIENCE

Most massive neutron star ever detected strains the limits of physics

By Ashley Strickland, CNN

Updated 0050 GMT (0850 HKT) September 17, 2019

nature astronomy
LETTERS
https://doi.org/10.1038/s41550-019-0880-2

Relativistic Shapiro delay measurements of an extremely massive millisecond pulsar

H. T. Cromartie[1*], E. Fonseca[2], S. M. Ransom[3], P. B. Demorest[4], Z. Arzoumanian[5], H. Blumer[6,7], P. R. Brook[6,7], M. E. DeCesar[8], T. Dolch[9], J. A. Ellis[10], R. D. Ferdman[11], E. C. Ferrara[12,13], N. Garver-Daniels[6,7], P. A. Gentile[6,7], M. L. Jones[6,7], M. T. Lam[6,7], D. R. Lorimer[6,7], R. S. Lynch[14], M. A. McLaughlin[6,7], C. Ng[15,16], D. J. Nice[8], T. T. Pennucci[17], R. Spiewak[18], I. H. Stairs[15], K. Stovall[4], J. K. Swiggum[19] and W. W. Zhu[20]

Despite its importance to our understanding of physics at supranuclear densities, the equation of state (EoS) of matter deep within neutron stars remains poorly understood. Millisecond pulsars (MSPs) are among the most useful astrophysical objects in the Universe for testing fundamental physics, and place some of the most stringent constraints on this high-density EoS. Pulsar timing—the process of accounting for every rotation of a pulsar over long time periods—can precisely measure a wide variety of physical phenomena, including those that allow the measurement of the masses of the components of a pulsar binary system[1]. One of these, called relativistic Shapiro delay[2], can yield precise masses for both an MSP and its companion; however, it is only easily observed in a small subset of high-precision, highly inclined (nearly edge-on) binary pulsar systems. By combining data from the North American Nanohertz Observatory for Gravitational Waves (NANOGrav) 12.5-yr data set with recent orbital-phase-specific observations using the Green Bank Telescope, we have measured the mass of the MSP J0740+6620 to be $2.14^{+0.10}_{-0.09}\,M_\odot$ (68.3% credibility interval; the 95.4% credibility interval is $2.14^{+0.20}_{-0.18}\,M_\odot$). It is highly likely to be the most massive neutron star yet observed, and serves as a strong constraint on the neutron star interior EoS.

Precise neutron star mass measurements are an effective way to constrain the EoS of the ultradense matter in neutron star interiors. Although radio pulsar timing cannot directly determine neutron star radii, the existence of pulsars with masses exceeding the maximum mass allowed by a given model can straightforwardly rule out that EoS.

In 2010, Demorest et al. reported the discovery of a $2\,M_\odot$ MSP, J1614−2230 (ref. [4]) (though the originally reported mass was $1.97\pm0.04\,M_\odot$, continued timing has led to a more precise mass measurement of $1.928\pm0.017\,M_\odot$ by Fonseca et al.[5]). This Shapiro-delay-enabled measurement disproved the plausibility of some hyperon, boson and free quark models in nuclear-density environments. In 2013, Antoniadis et al. used optical techniques in combination with pulsar timing to yield a mass measurement of $2.01\pm0.04\,M_\odot$ for the pulsar J0348+0432 (ref. [6]). These two observational results (along with others[7]) encouraged a reconsideration of the canonical $1.4\,M_\odot$ neutron star. Gravitational-wave astrophysics has also begun to provide EoS constraints; for example, the Laser Interferometer Gravitational-Wave Observatory (LIGO) detection of a double neutron star merger constrains permissible EoSs, suggesting that the upper limit on neutron star mass is $2.17\,M_\odot$ (90% credibility[8]). Though the existence of extremely massive ($>2.4\,M_\odot$) neutron stars has been suggested through optical spectroscopic

Massive Neutron Stars

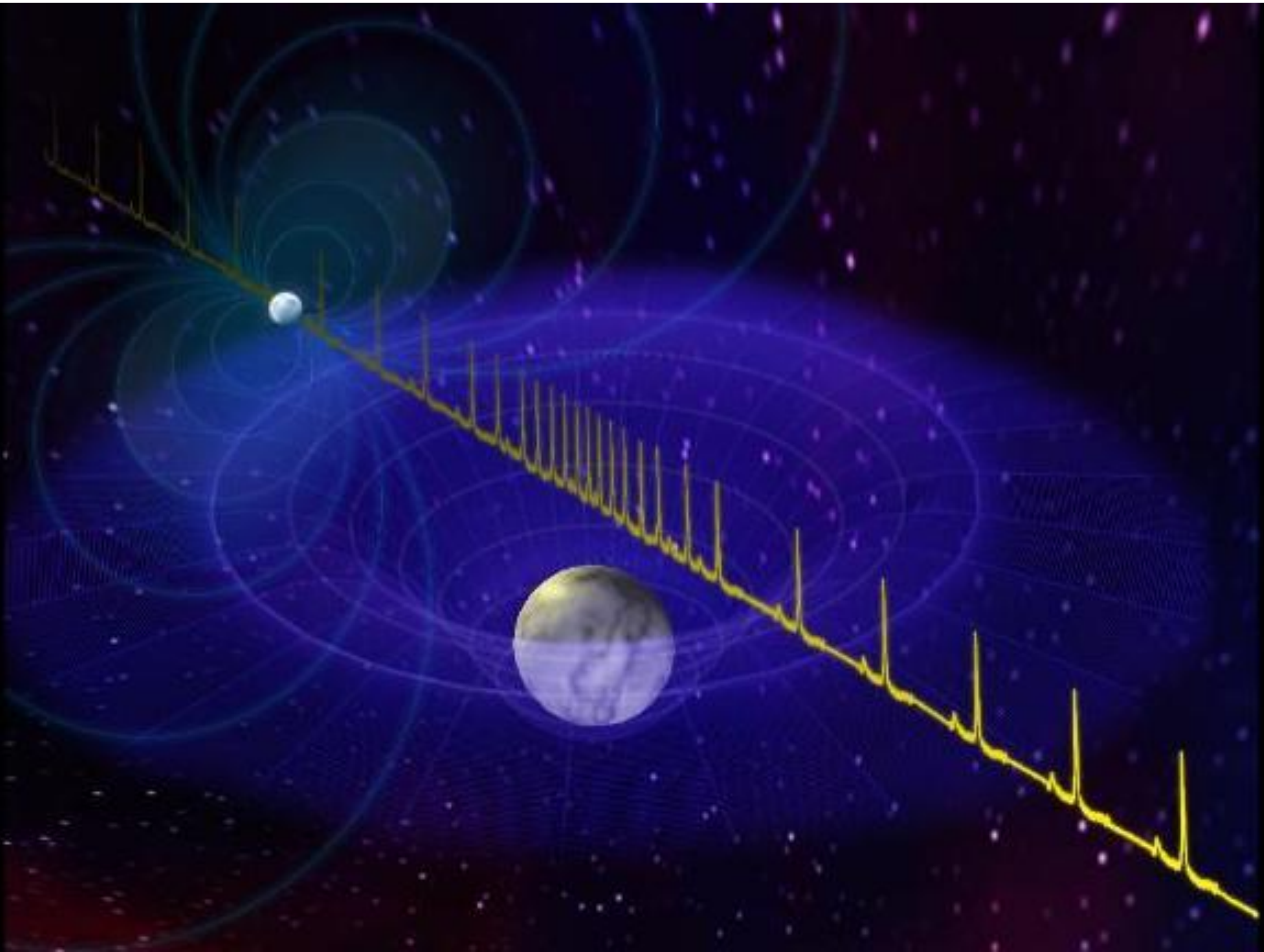

PSR J1614-2230

A precise AND large mass measurement

Shapiro delay:

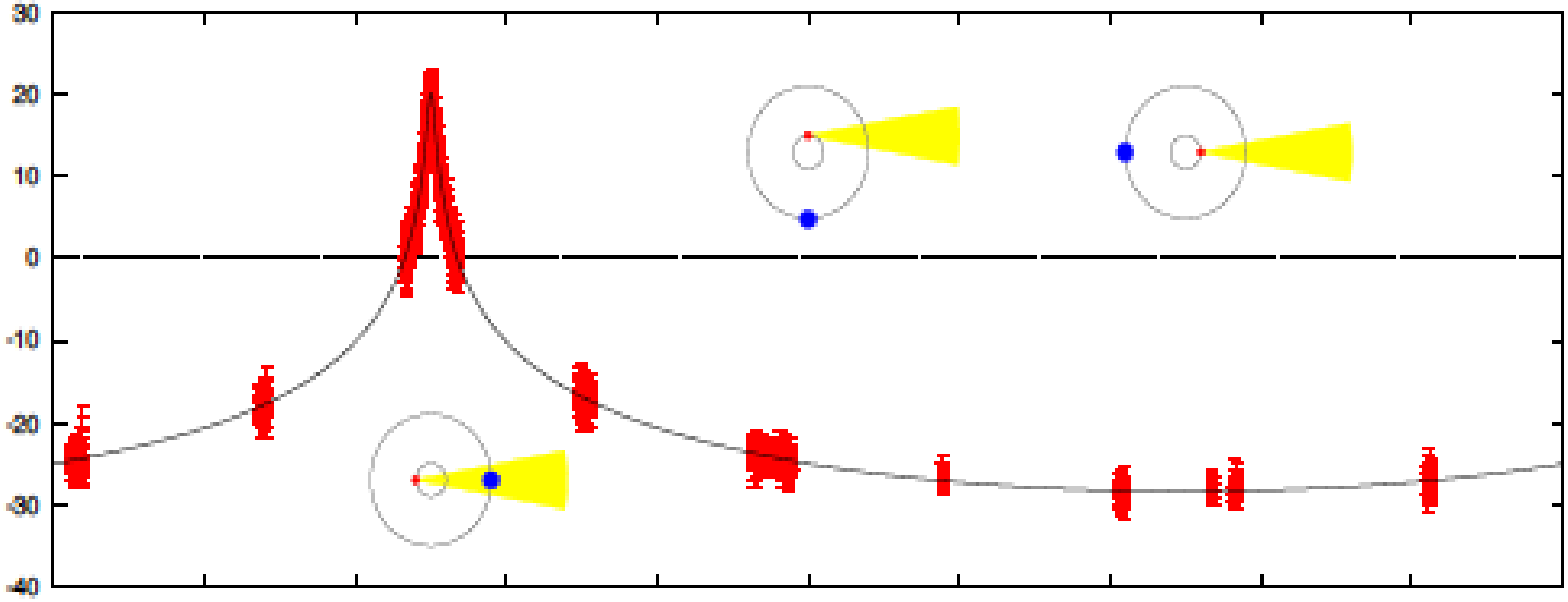

Massive Neutron Stars

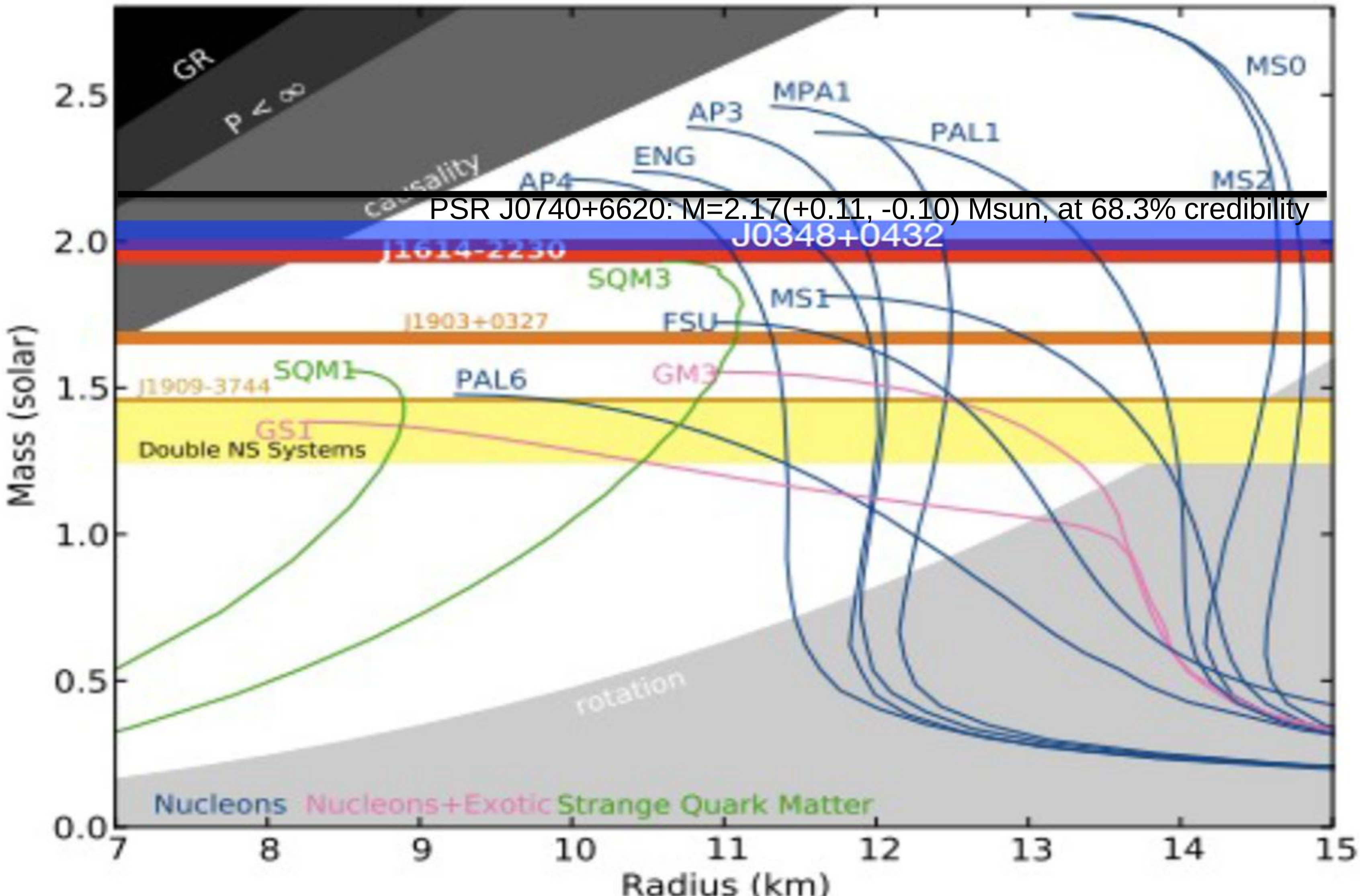

Critical Endpoint in QCD

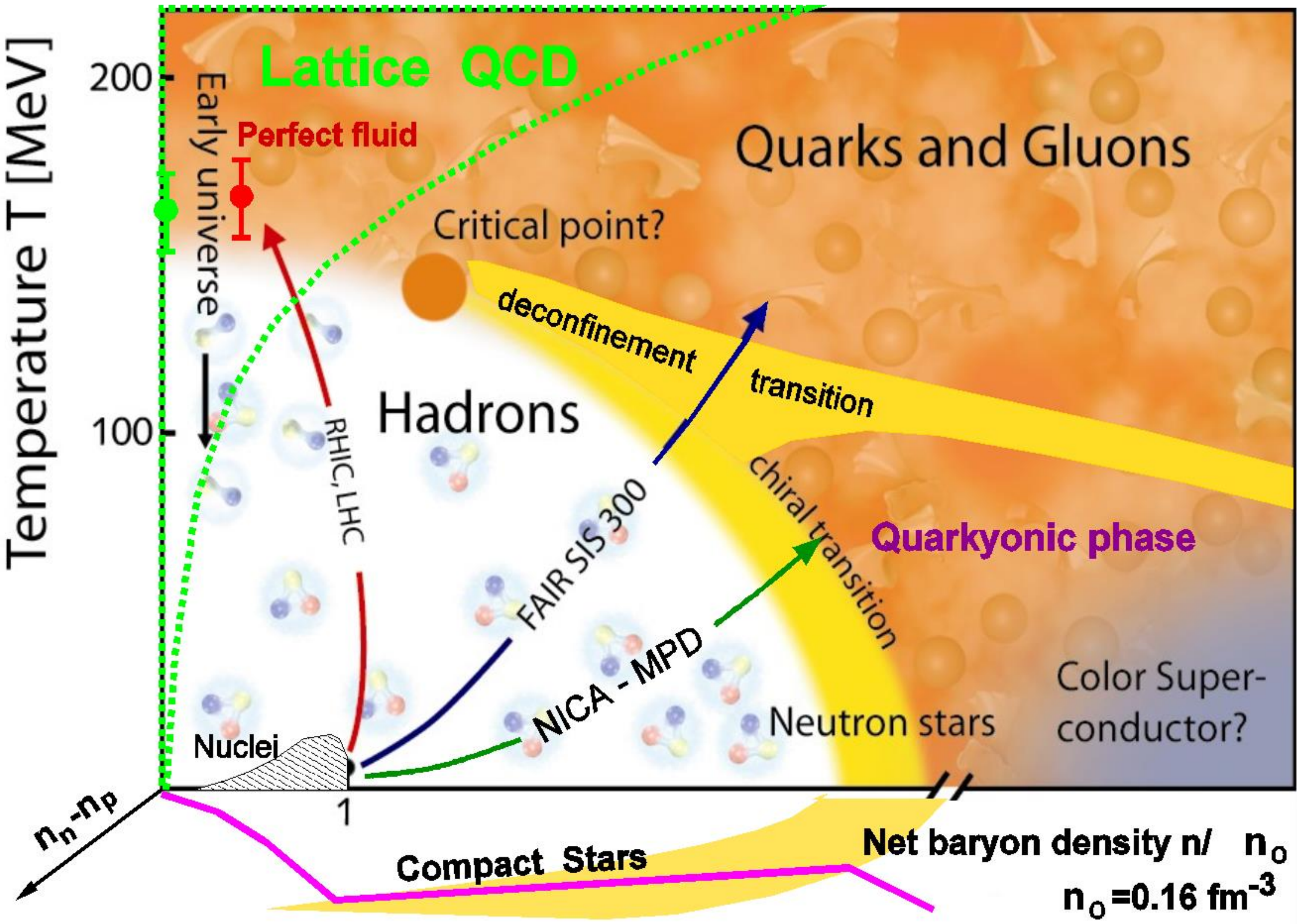

Compact Star Mass Twins and the AHP scheme

- First order PT can lead to a stable branch of hybrid stars with quark matter cores which, depending on the size of the "latent heat" (jump in energy density), can even be disconnected from the hadronic one by an unstable branch → "**third family of CS**".

- Measuring two **disconnected populations** of compact stars in the M-R diagram would represent **the detection of a first order phase transition** in compact star matter and thus the indirect proof for the existence of a **critical endpoint (CEP) in the QCD phase diagram**!

Alford, Han, Prakash,
Phys. Rev. D 88, 083013 (2013)
arxiv:1302.4732

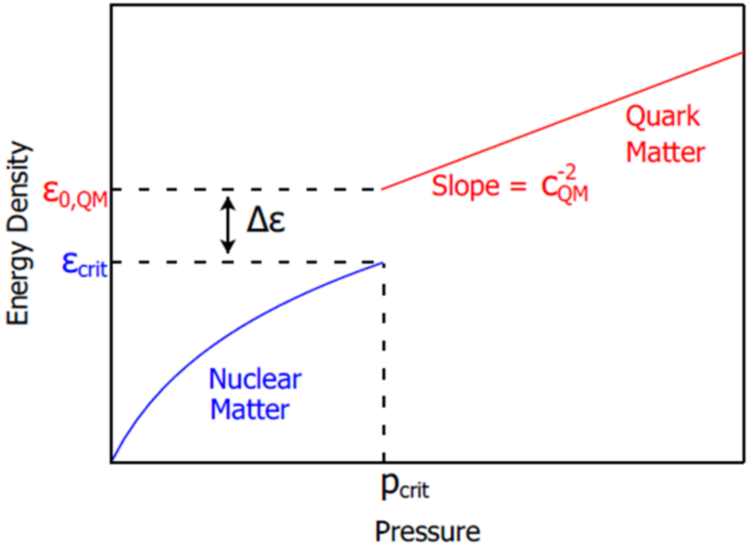

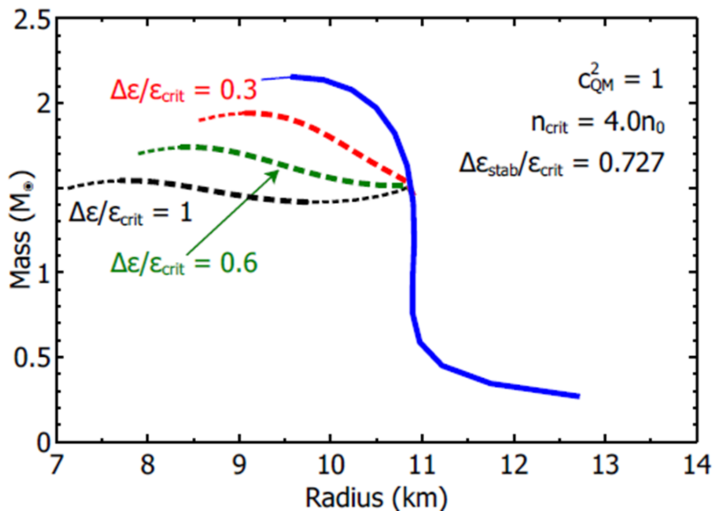

Piecewise polytrope EoS

Hebeler et al., ApJ 773, 11 (2013)

$$P_i(n) = \kappa_i n^{\Gamma_i}$$

$$i = 1 \;:\; n_1 \le n \le n_{12}$$
$$i = 2 \;:\; n_{12} \le n \le n_{23}$$
$$i = 3 \;:\; n \ge n_{23}\;,$$

Here, 1st order PT in region 2:

$$\Gamma_2 = 0 \text{ and } P_2 = \kappa_2 = P_{\rm crit}$$

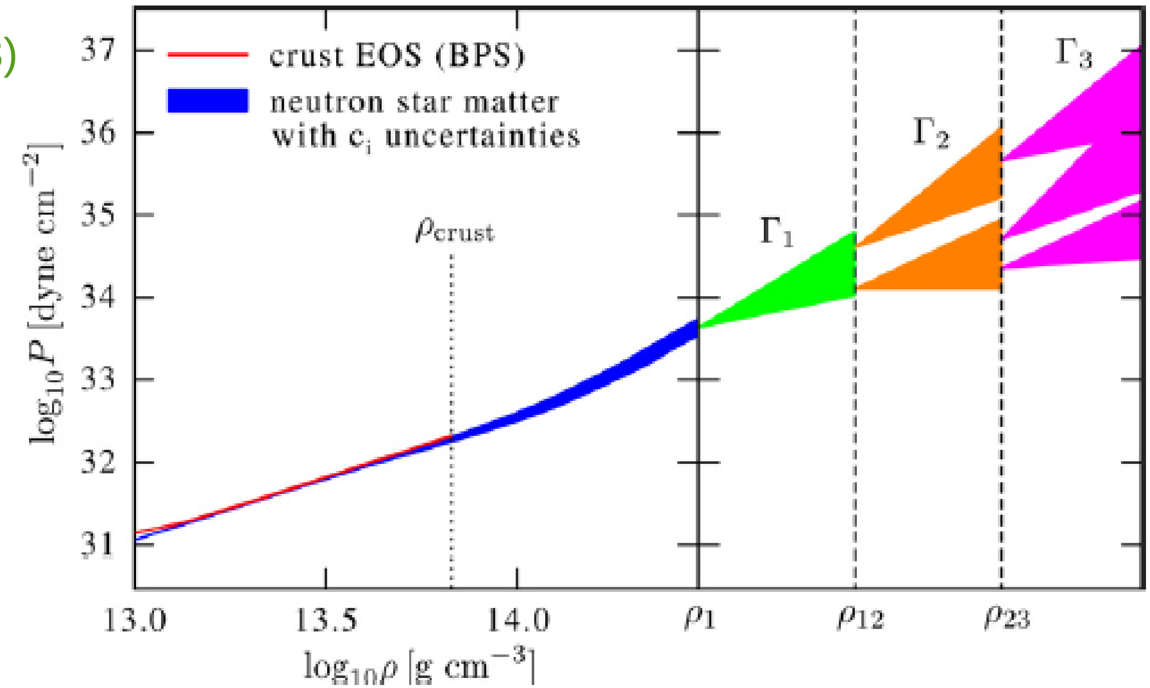

$$P(n) \;=\; n^2 \frac{d(\varepsilon(n)/n)}{dn},$$

$$\varepsilon(n)/n \;=\; \int dn\, \frac{P(n)}{n^2} = \int dn\, \kappa n^{\Gamma-2} = \frac{\kappa\, n^{\Gamma-1}}{\Gamma-1} + C,$$

$$\mu(n) \;=\; \frac{P(n)+\varepsilon(n)}{n} = \frac{\kappa\,\Gamma}{\Gamma-1} n^{\Gamma-1} + m_0,$$

$$n(\mu) \;=\; \left[(\mu - m_0)\frac{\Gamma-1}{\kappa\Gamma}\right]^{1/(\Gamma-1)}$$

$$P(\mu) \;=\; \kappa\left[(\mu - m_0)\frac{\Gamma-1}{\kappa\Gamma}\right]^{\Gamma/(\Gamma-1)}$$

Maxwell construction:

$$P_1(\mu_{\rm crit}) \;=\; P_3(\mu_{\rm crit}) = P_{\rm crit}$$
$$\mu_{\rm crit} \;=\; \mu_1(n_{12}) = \mu_3(n_{23})$$

Seidov criterion for instability: $\dfrac{\Delta\varepsilon}{\varepsilon_{\rm crit}} \ge \dfrac{1}{2} + \dfrac{3}{3}\dfrac{P_{\rm crit}}{\varepsilon_{\rm crit}}$

Compact Star Twins

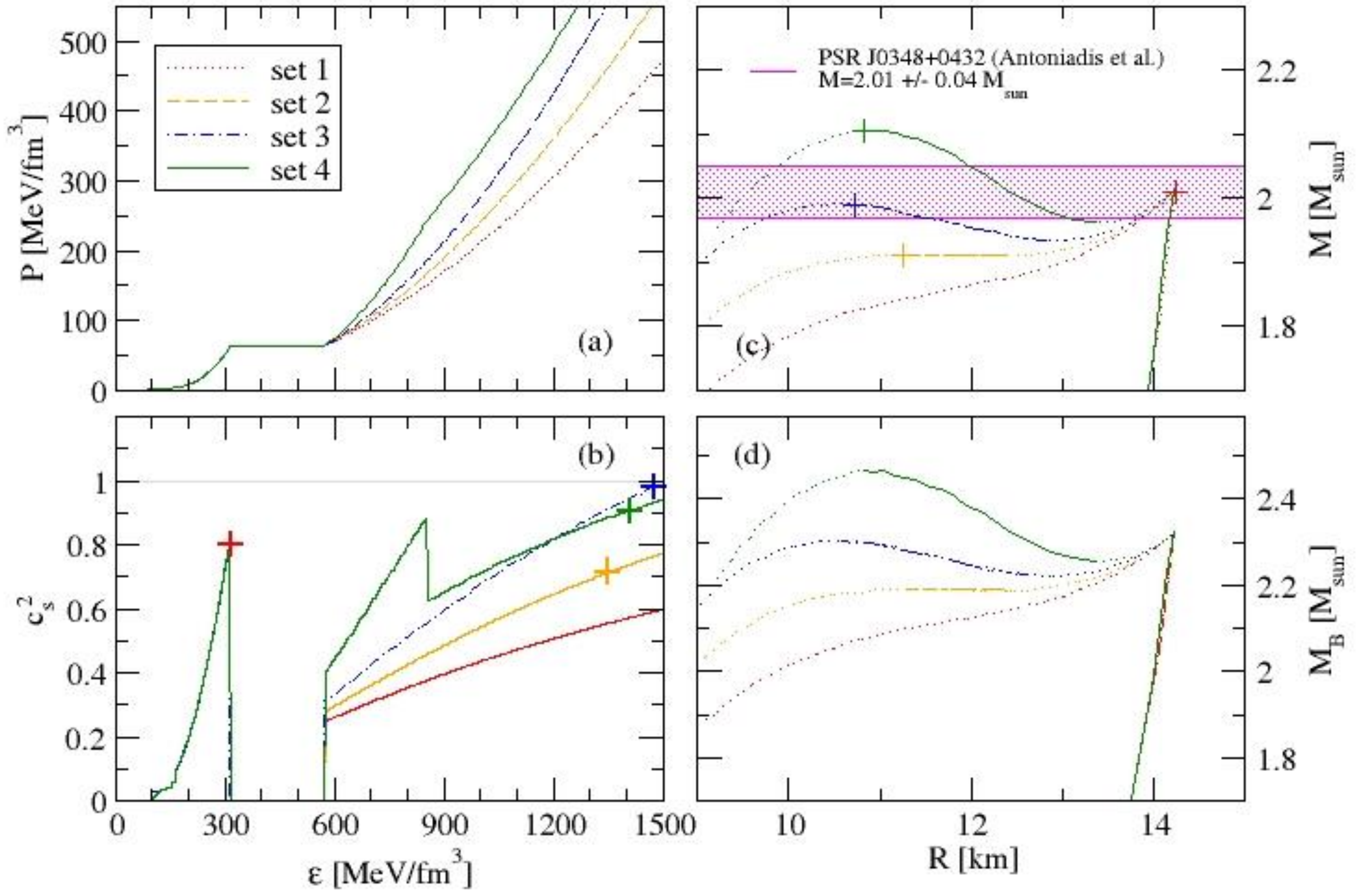

Alvarez-Castillo, Blaschke (2017)
High mass twins from multi-polytrope equations of state
arXiv: 1703.02681v2, Phys. Rev. C 96, 045809 (2017)

Multi-messenger Astronomy

Hulse-Taylor pulsar – binary system

PSR B1913+16 (now J1915+1606)

Nobel Prize for Hulse and Taylor (1993)

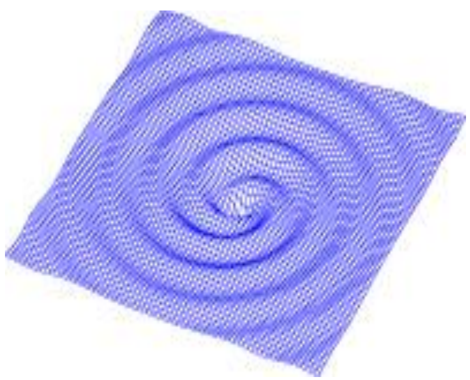

Excellent confirmation of Einstein theory of GW emission by observation of period decay

Anatomy of the GW signal

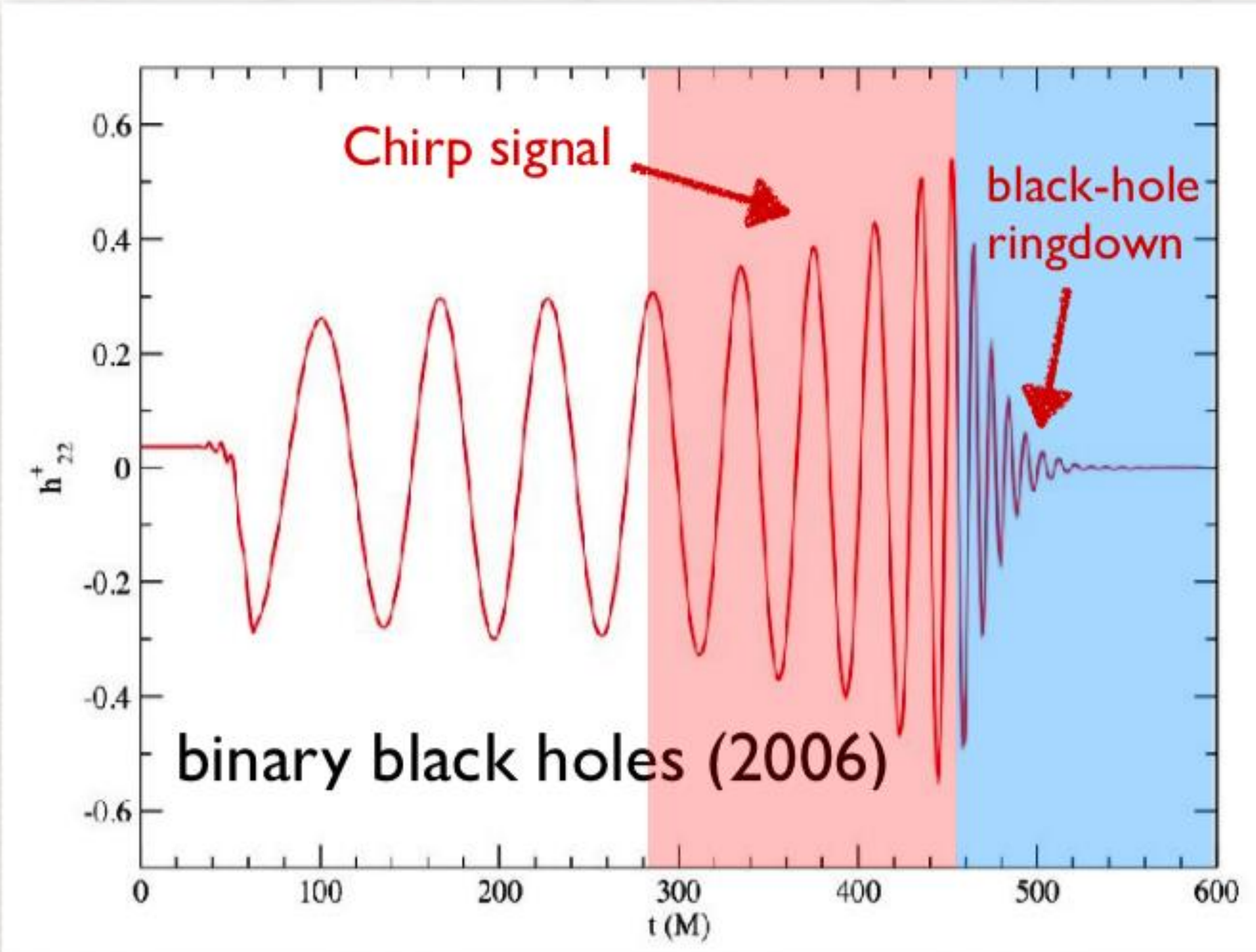

Direct measurement of gravitational waves – merging of two massive black holes (2015)

First detection of gravitational waves
September 14, 2015 at 5:51 a.m. EDT
(LIGO Collaboration)

Source at 410(18) Mpc [z=0.09(4)]

Initial black hole masses:
36(5) Mo and 29(4) Mo
Final black hole mass:
62(4) Mo

Energy release in gravitational waves
3.0(5) Mo c^2

Phys. Rev. Lett. 116, 061102 (2016)

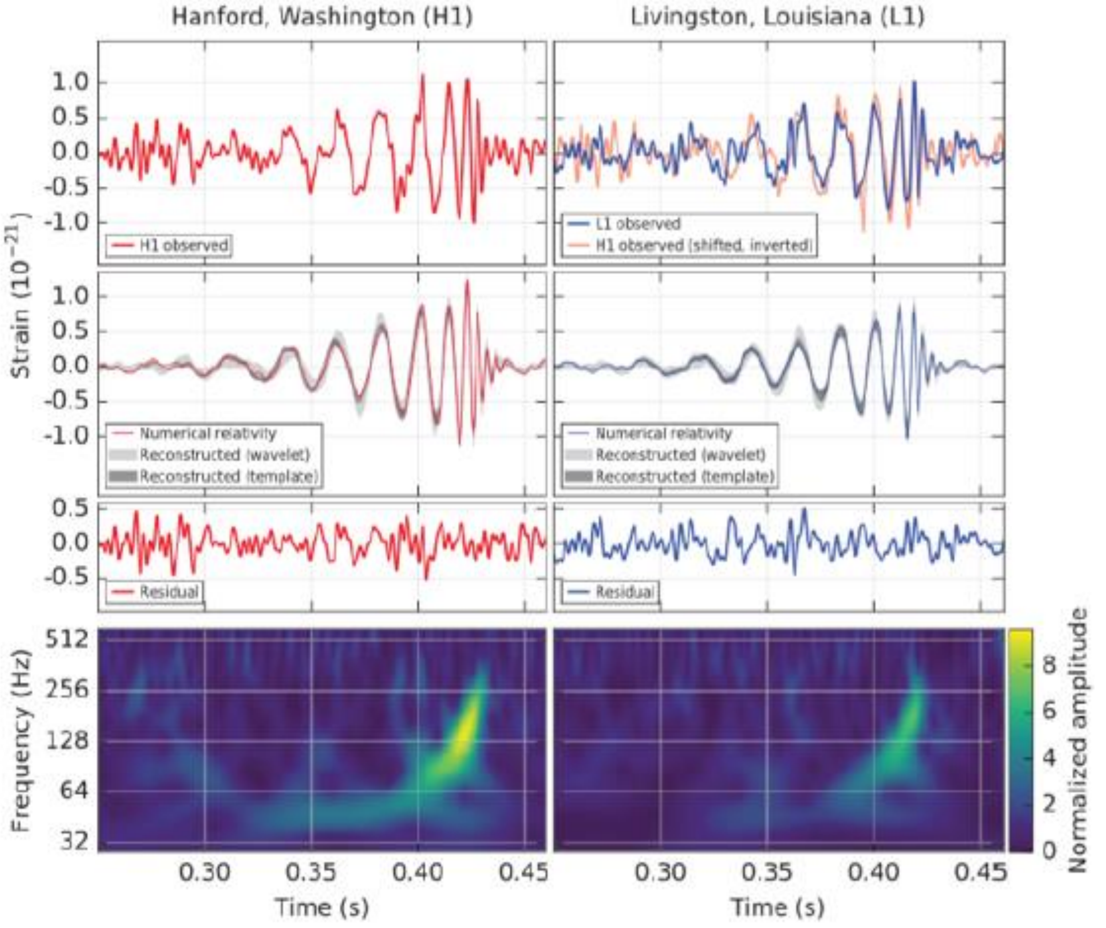

Nobel Prize Physics 2017 !! Rainer Weiss, Barry C. Barish, Kip Thorne

GW170817: Neutron Star Merger

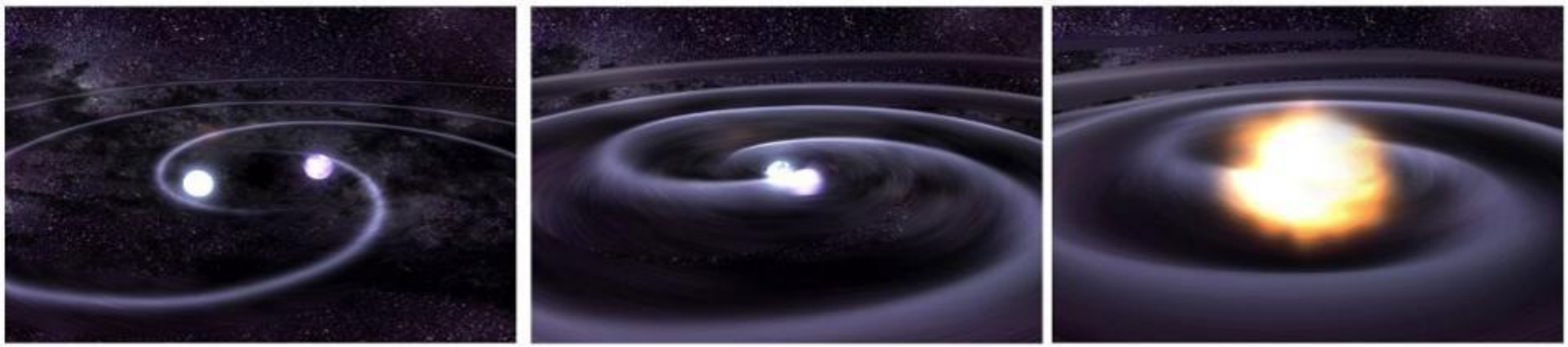

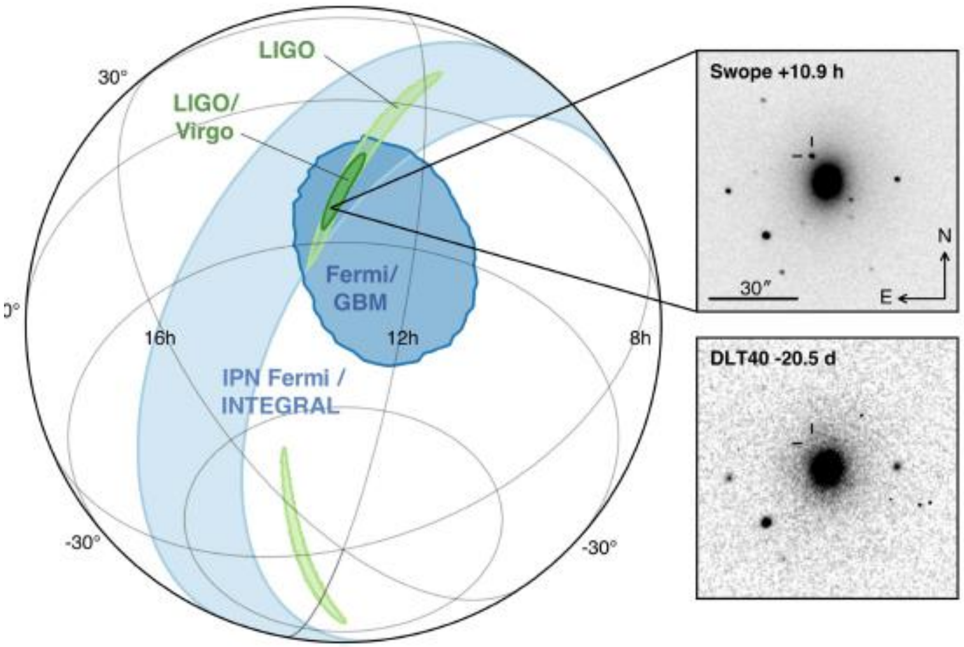

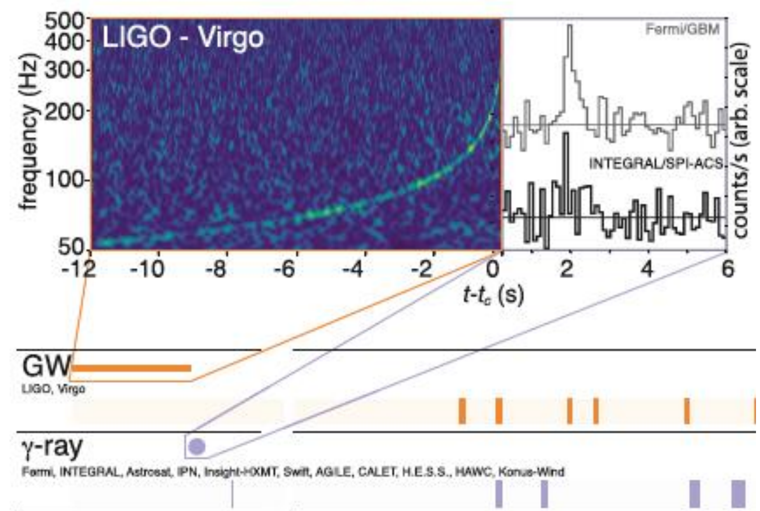

*) B.P. Abbott et al. [LIGO/Virgo Collab.], PRL 119, 161101 (2017); ApJLett 848, L12 (2017)

Anatomy of the GW signal

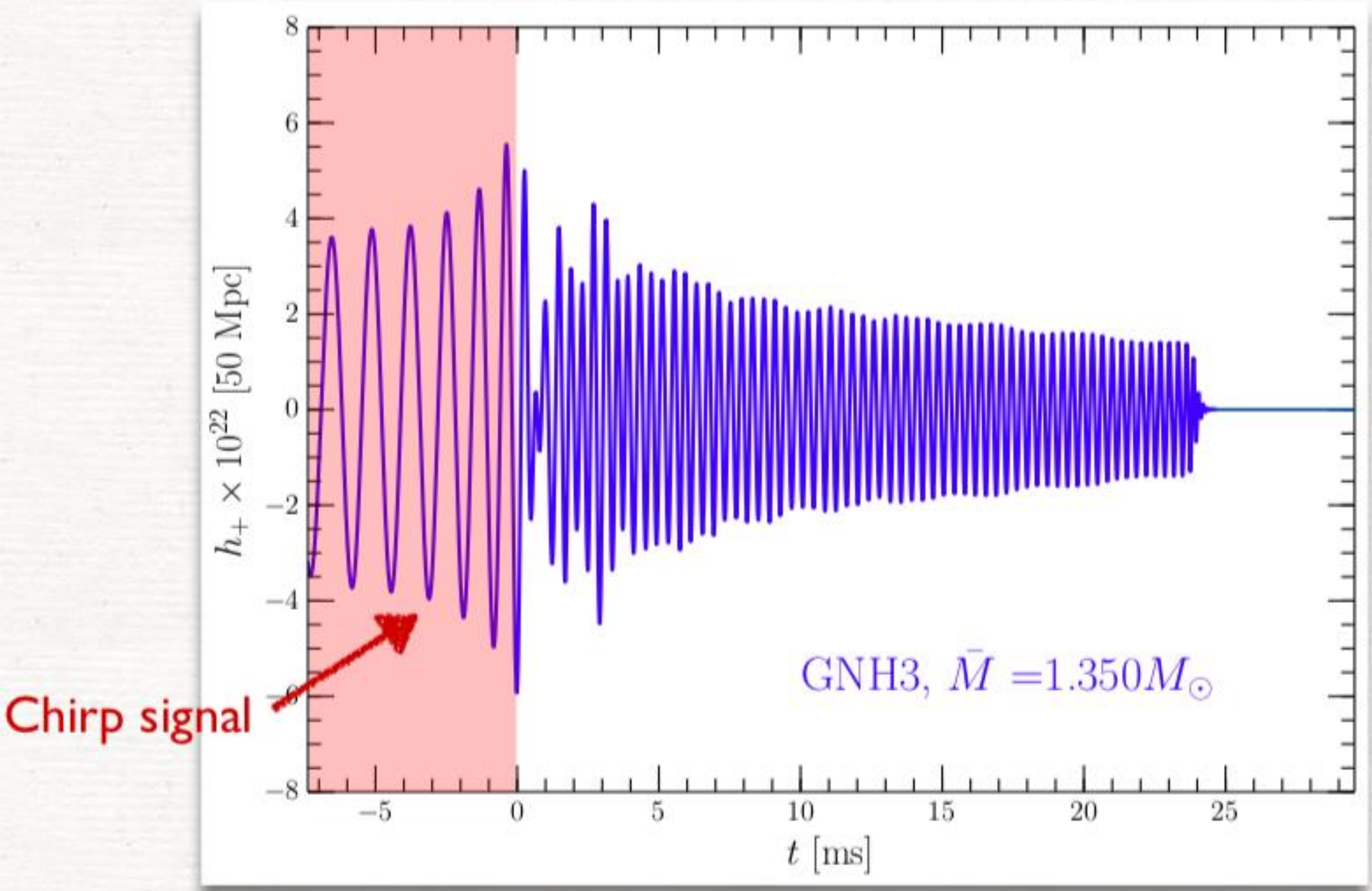

Implications from GW170817

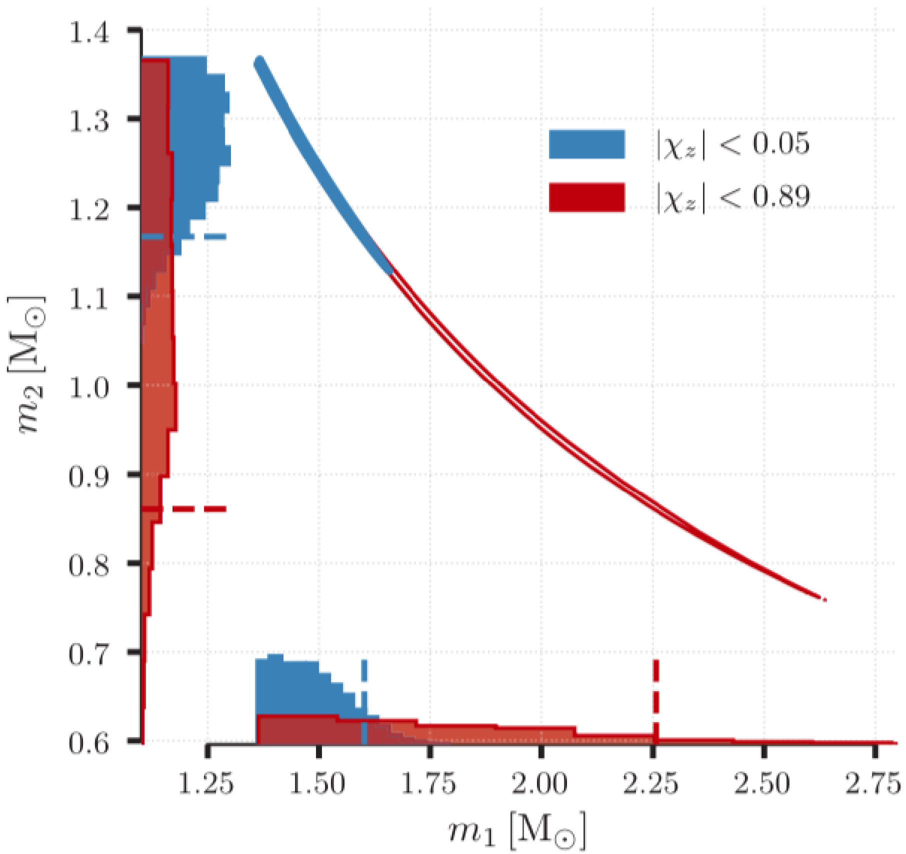

GW170817: Observation of Gravitational Waves from a Binary Neutron Star Inspiral
B. P. Abbott et al. arXiv:1712.00451

What can we learn from the inspiral II

- Waveforms incl. finite-size effects are described by tidal deformability (how a star reacts on an external tidal field)
- Offer possibility to constrain EoS because tidal deformability depends on EoS

$$\Lambda \equiv \frac{2}{3} k_2 \left(\frac{R}{M} \right)^5$$

- Corresponding to ~10 % error in radius R for nearby events (<100Mpc) (e.g. Read et al. 2013)
- Note: faithful templates to be constructed

R/M compactness (EoS dependent)

k_2 tidal love number (EoS dependent)

Computing the love number/tidal deformability

Extension of a standard TOV solver (i.e. numerically an integration of coupled ODEs):

Ansatz for the metric including a l=2 perturbation

$$\begin{aligned} ds^2 &= -e^{2\Phi(r)}\left[1+H(r)Y_{20}(\theta,\varphi)\right]dt^2 \\ &\quad +e^{2\Lambda(r)}\left[1-H(r)Y_{20}(\theta,\varphi)\right]dr^2 \\ &\quad +r^2\left[1-K(r)Y_{20}(\theta,\varphi)\right]\left(d\theta^2+\sin^2\theta d\varphi^2\right) \end{aligned}$$

Following Hinderer et al. 2010

Integrate standard TOV system:

$$\begin{aligned} e^{2\Lambda} &= \left(1-\frac{2m_r}{r}\right)^{-1}, \\ \frac{d\Phi}{dr} &= -\frac{1}{\epsilon+p}\frac{dp}{dr}, \\ \frac{dp}{dr} &= -(\epsilon+p)\frac{m_r+4\pi r^3 p}{r(r-2m_r)}, \\ \frac{dm_r}{dr} &= 4\pi r^2\epsilon. \end{aligned}$$

EoS to be provided ε(p)

And additional eqs. for perturbations:

$$\begin{aligned} \frac{dH}{dr} &= \beta \qquad (11) \\ \frac{d\beta}{dr} &= 2\left(1-2\frac{m_r}{r}\right)^{-1}H\left\{-2\pi\left[5\epsilon+9p+f(\epsilon+p)\right]\right. \\ &\qquad \left.+\frac{3}{r^2}+2\left(1-2\frac{m_r}{r}\right)^{-1}\left(\frac{m_r}{r^2}+4\pi rp\right)^2\right\} \\ &\quad +\frac{2\beta}{r}\left(1-2\frac{m_r}{r}\right)^{-1}\left\{-1+\frac{m_r}{r}+2\pi r^2(\epsilon-p)\right\}. \end{aligned}$$

(K(r) given by H(r))

Note: Although multidimensional problem – computation in 1D since absorbed in Y20

Love number

$$y = \frac{R\,\beta(R)}{H(R)}$$

$$\begin{aligned}
k_2 \;=\; & \frac{8C^5}{5}(1-2C)^2[2+2C(y-1)-y] \\
& \times\Big\{2C[6-3y+3C(5y-8)] \\
& \quad +4C^3[13-11y+C(3y-2)+2C^2(1+y)] \\
& \quad +3(1-2C)^2[2-y+2C(y-1)]\ln(1-2C)\Big\}^{-1}
\end{aligned}$$

where $C = M/R$ is the compactness of the star.

Implications from GW170817

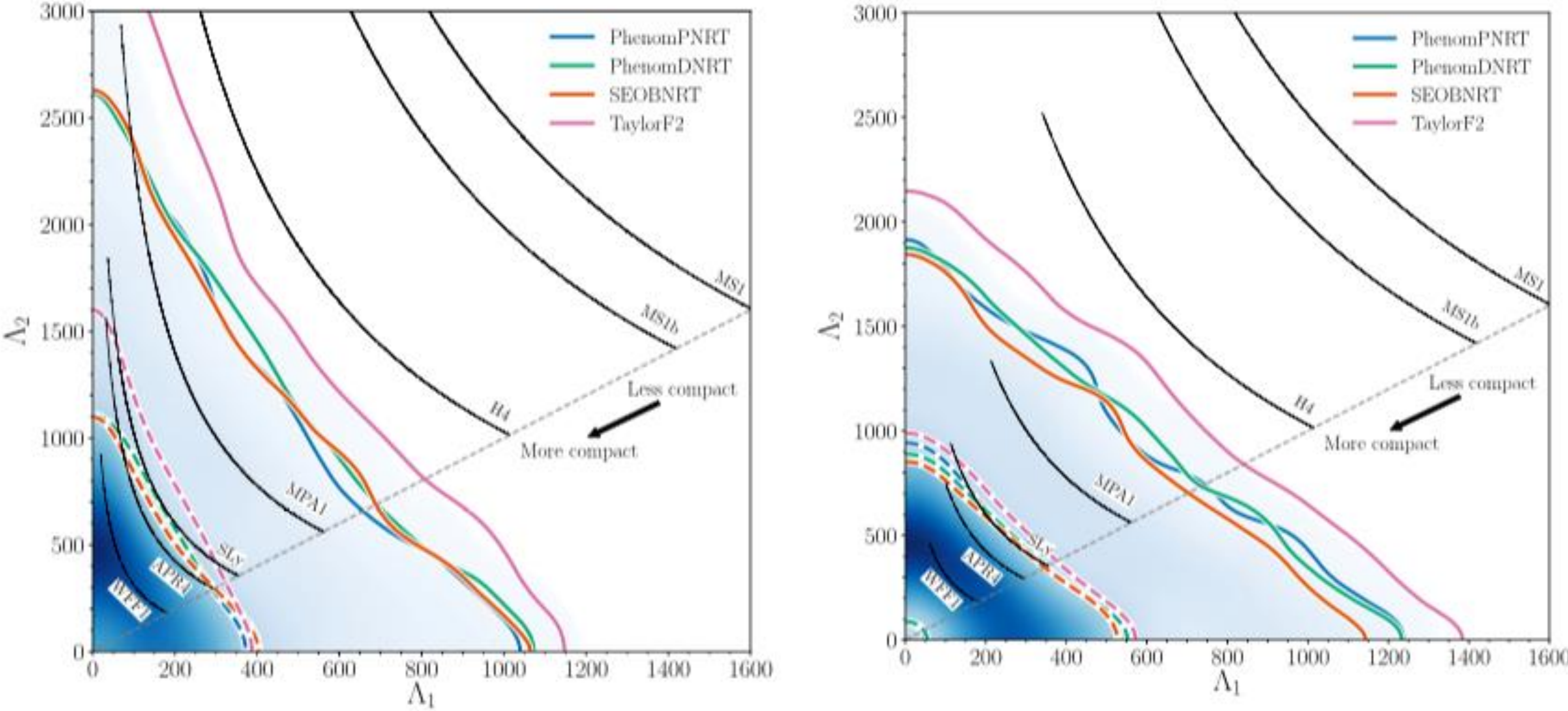

Properties of the Binary Star Merger GW170817
B. P. Abbott et al., Phys. Rev. X 9, 011001 (2019)

Implications from GW170817

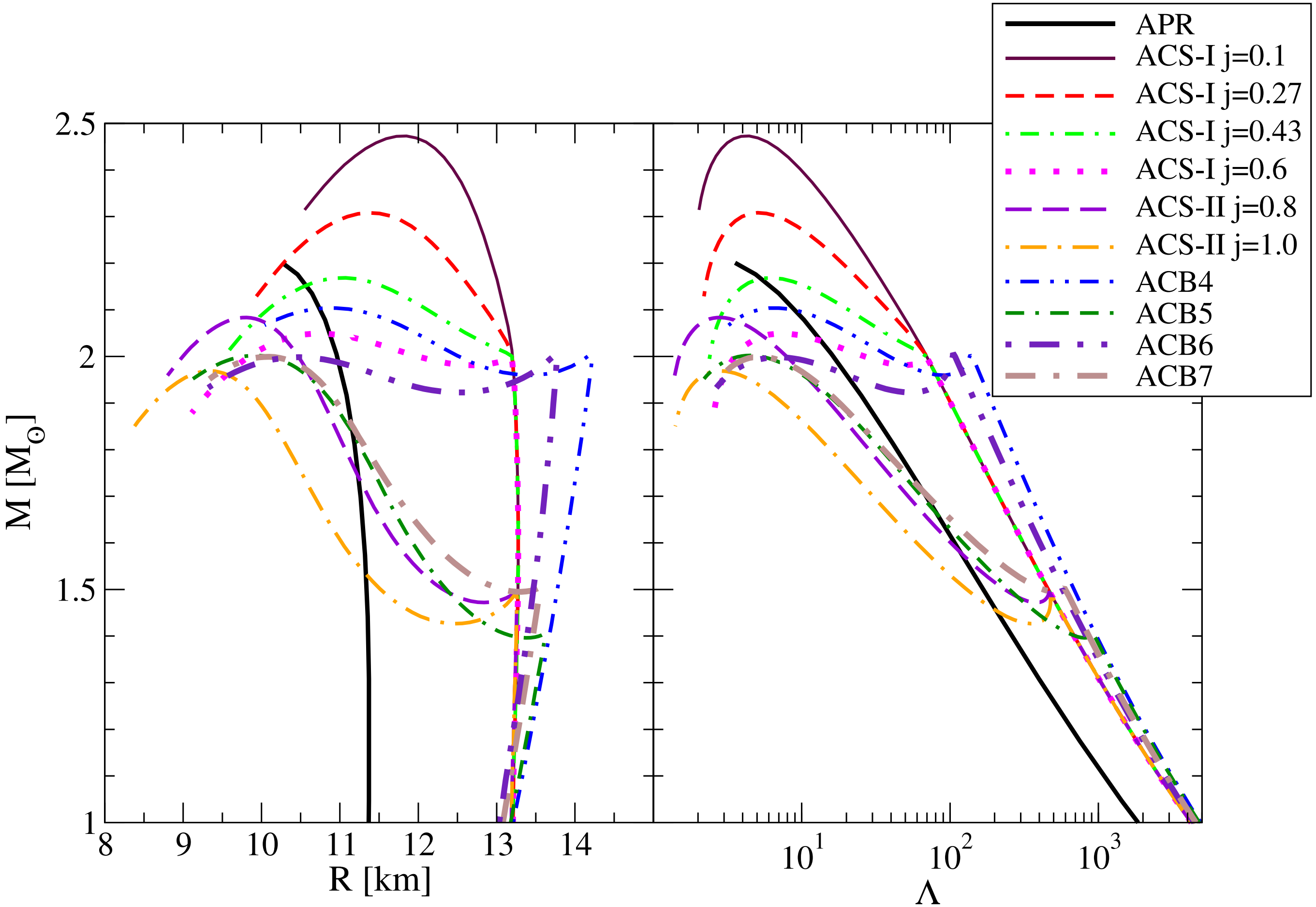

Vasileios Paschalidis, Kent Yagi, David Alvarez-Castillo, David B. Blaschke, Armen Sedrakian
Phys. Rev. D 97, 084038 (2018), arXiv:1712.00451

Implications from GW170817

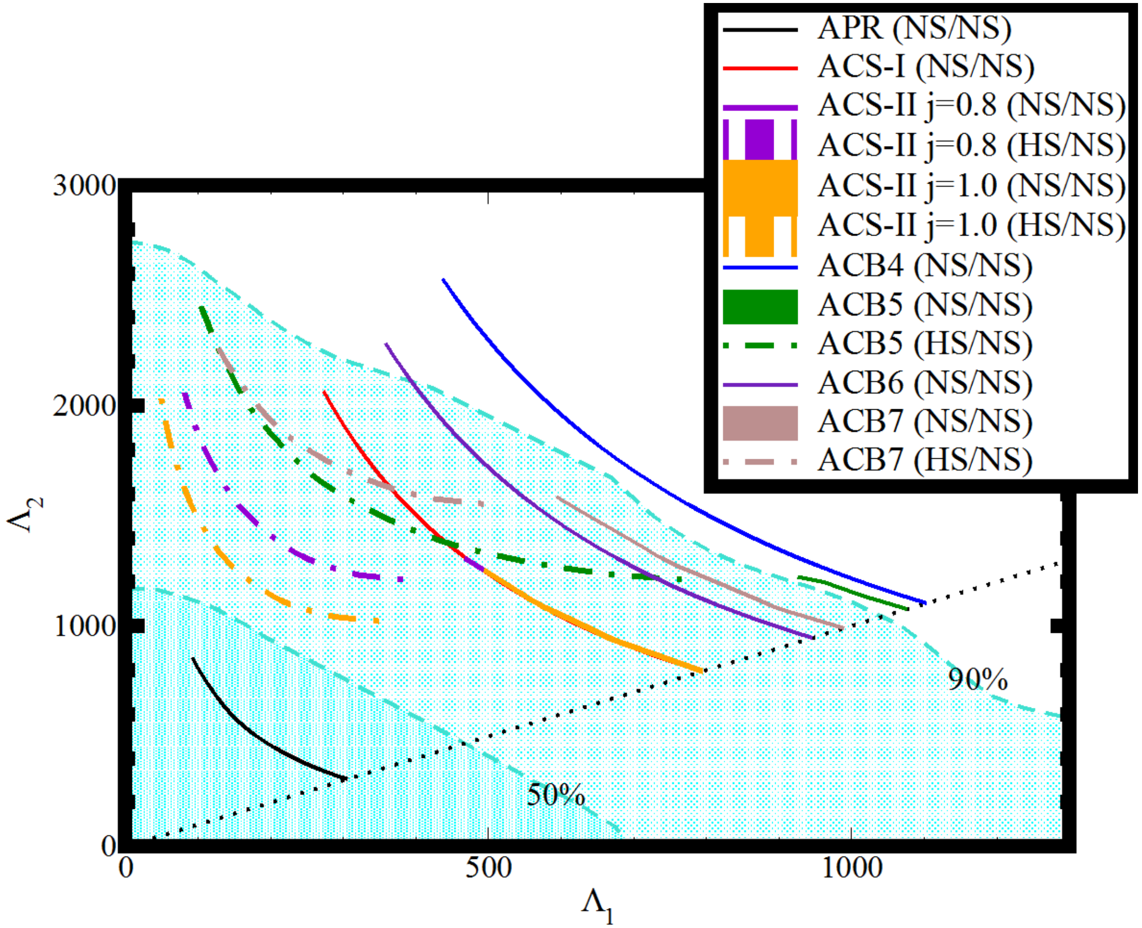

Vasileios Paschalidis, Kent Yagi, David Alvarez-Castillo, David B. Blaschke, Armen Sedrakian
Phys. Rev. D 97, 084038 (2018), arXiv:1712.00451

Perspectives for new Instruments?

THE FUTURE: SKA - SQUARE KILOMETER ARRAY

Measurement of Spin Precession of a Pulsar

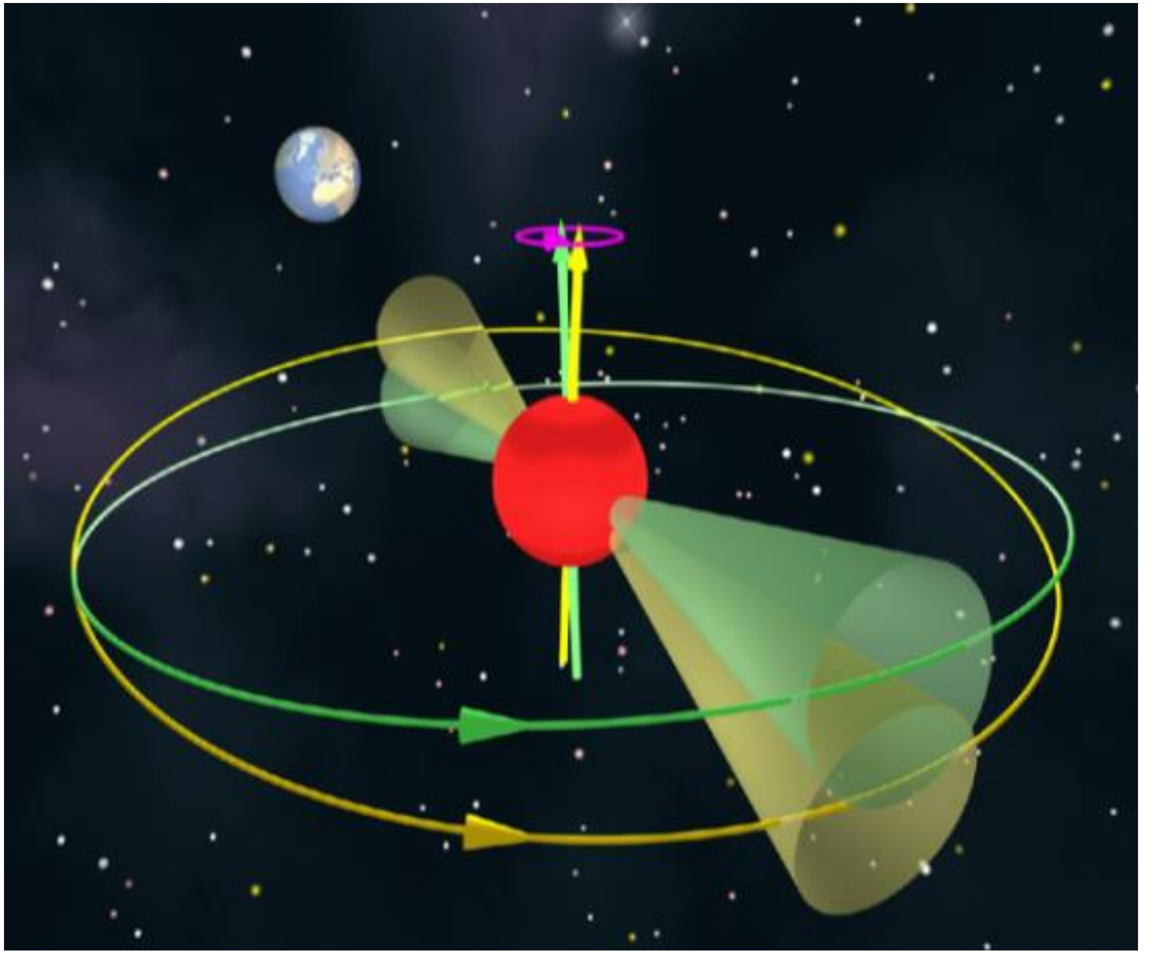

Moments of Inertia

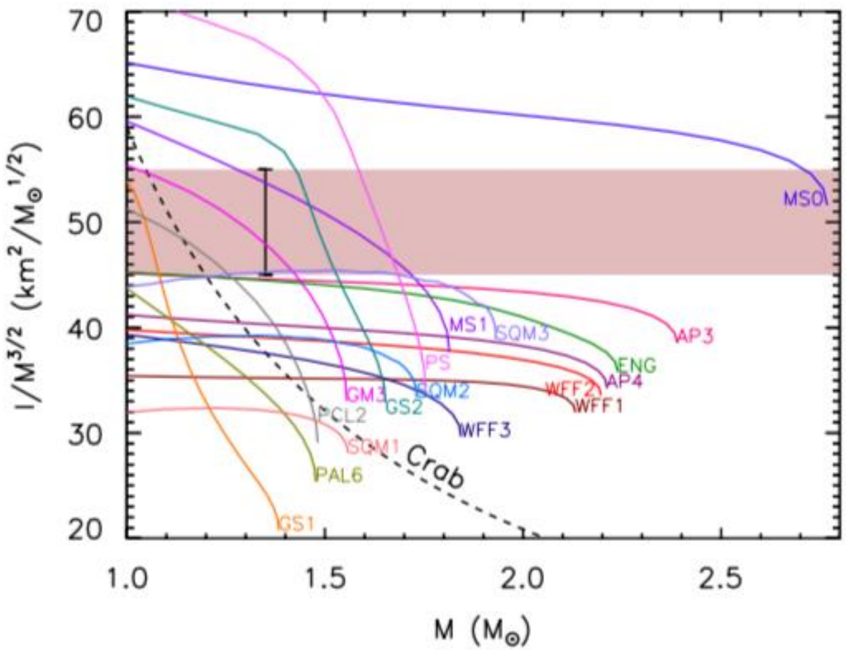

Fig. 9. The moment of inertia scaled by $M^{3/2}$ as a function of stellar mass M for EOSs described in [6]. The shaded band illustrates a $\pm 10\%$ error on a hypothetical $I/M^{3/2}$ measurement with centroid $50\,\mathrm{km}^2\,\mathrm{M}_\odot^{-1/2}$; the error bar shows the specific case in which the mass is $1.34\,\mathrm{M}_\odot$ with essentially no error. The dashed curve labelled "Crab" is the lower limit derived by [123] for the Crab pulsar.

$$I \simeq \frac{J}{1+2GJ/R^3c^2}, \quad J = \frac{8\pi}{3}\int_0^R r^4\left(\rho + \frac{p}{c^2}\right)\Lambda dr, \quad \Lambda = \frac{1}{1-2Gm/rc^2}$$

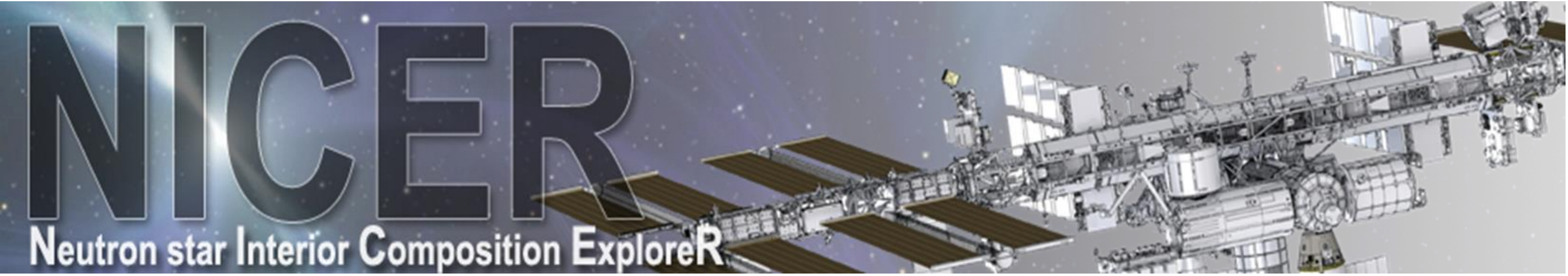

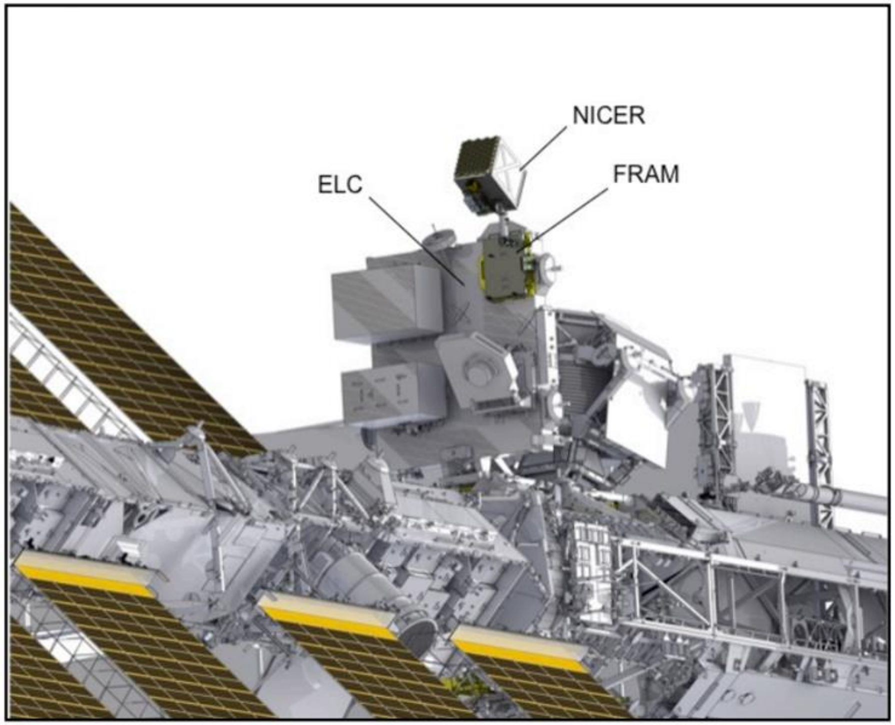

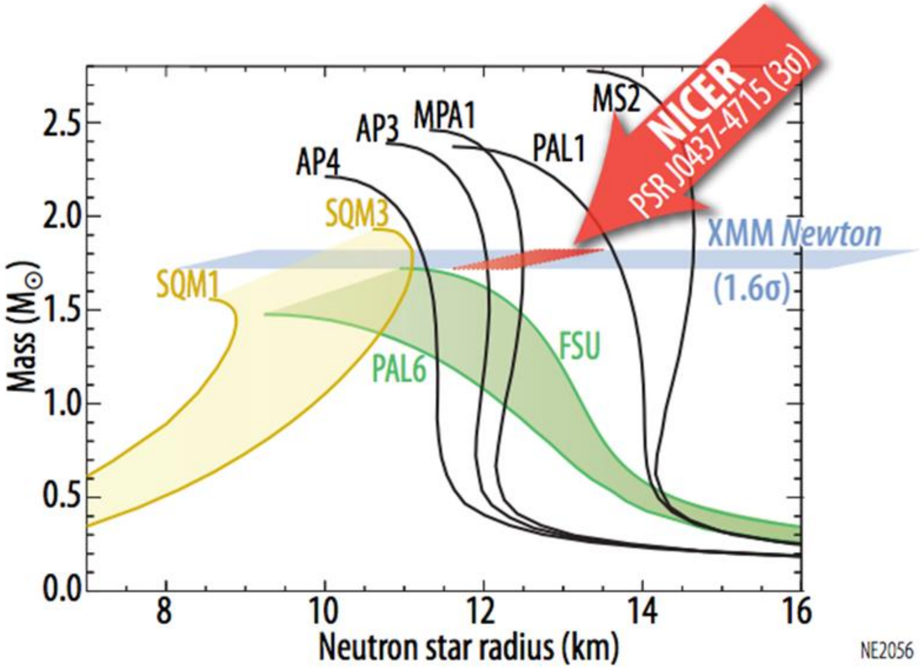

NICER 2017

Gendreau, K. C., Arzoumanian, Z., & Okajima, T. 2012, Proc. SPIE, 8443, 844313

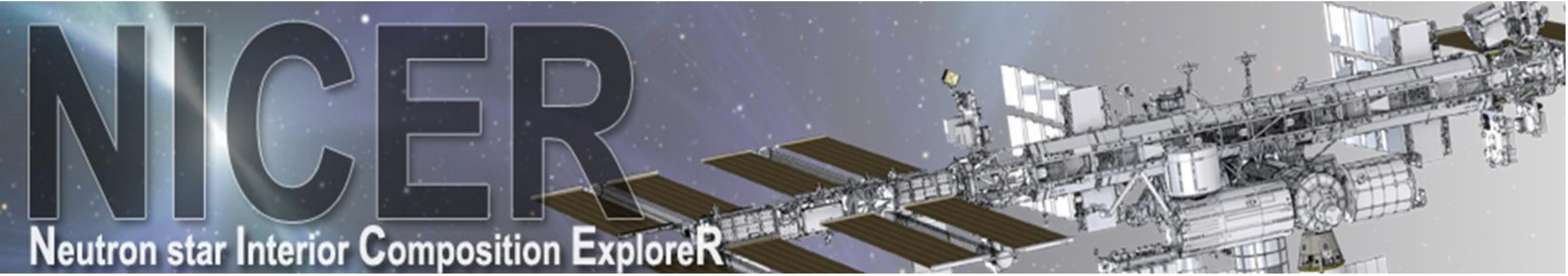
NICER
Neutron star Interior Composition ExploreR

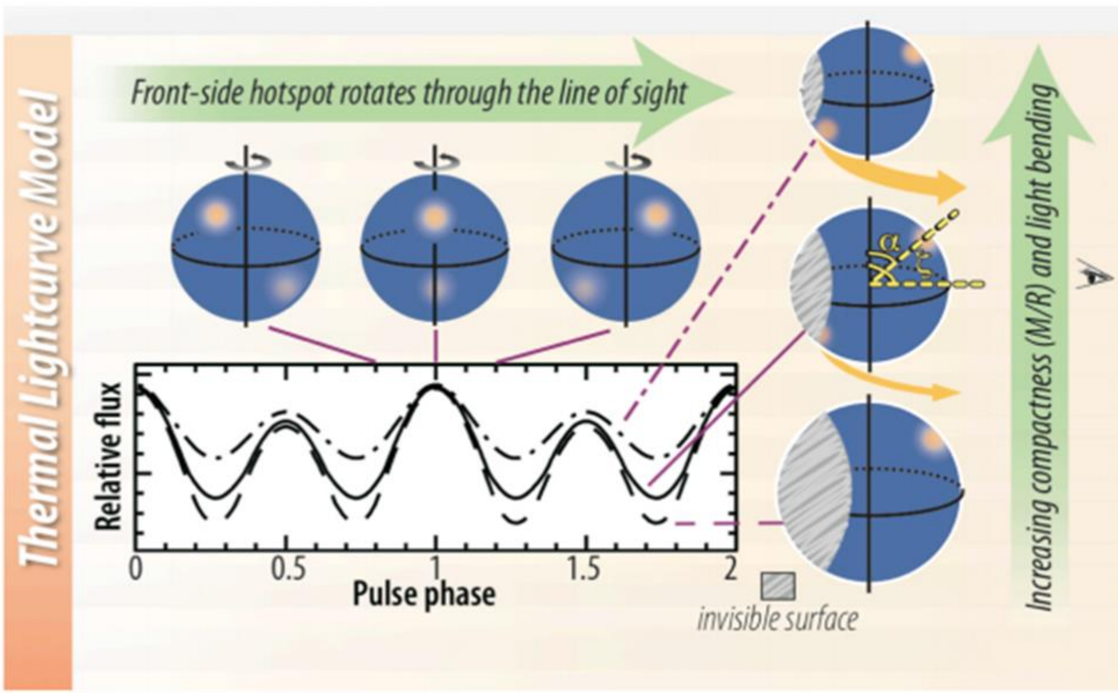
Thermal Lightcurve Model
Front-side hotspot rotates through the line of sight
Increasing compactness (M/R) and light bending
Relative flux
0
0.5
1
1.5
2
Pulse phase
invisible surface
α
ξ

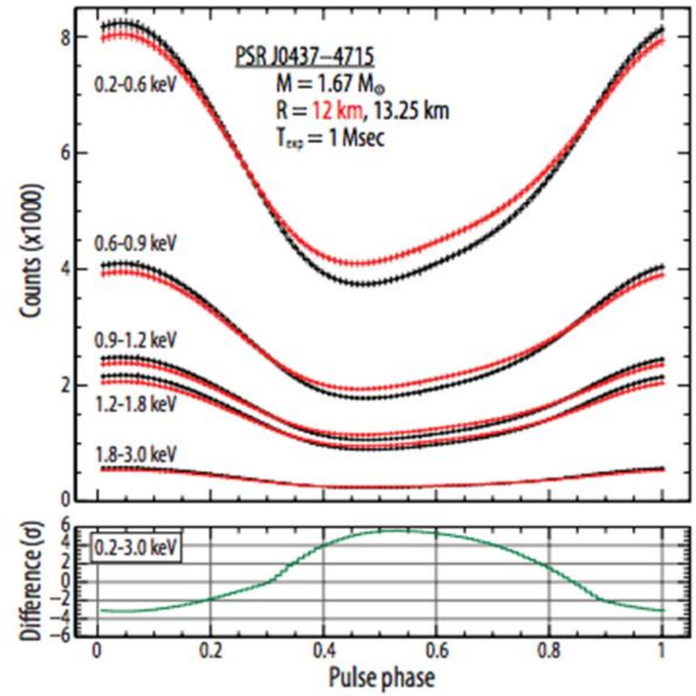
PSR J0437−4715
M = 1.67 M⊙
R = 12 km, 13.25 km
T exp = 1 Msec
0.2-0.6 keV
0.6-0.9 keV
0.9-1.2 keV
1.2-1.8 keV
1.8-3.0 keV
Counts (x1000)
8
6
4
2
0
Difference (σ)
0.2-3.0 keV
6
4
2
0
−2
−4
−6
0
0.2
0.4
0.6
0.8
1
Pulse phase

Hot Spots

Implications from GW170817
Nonlocal NJL

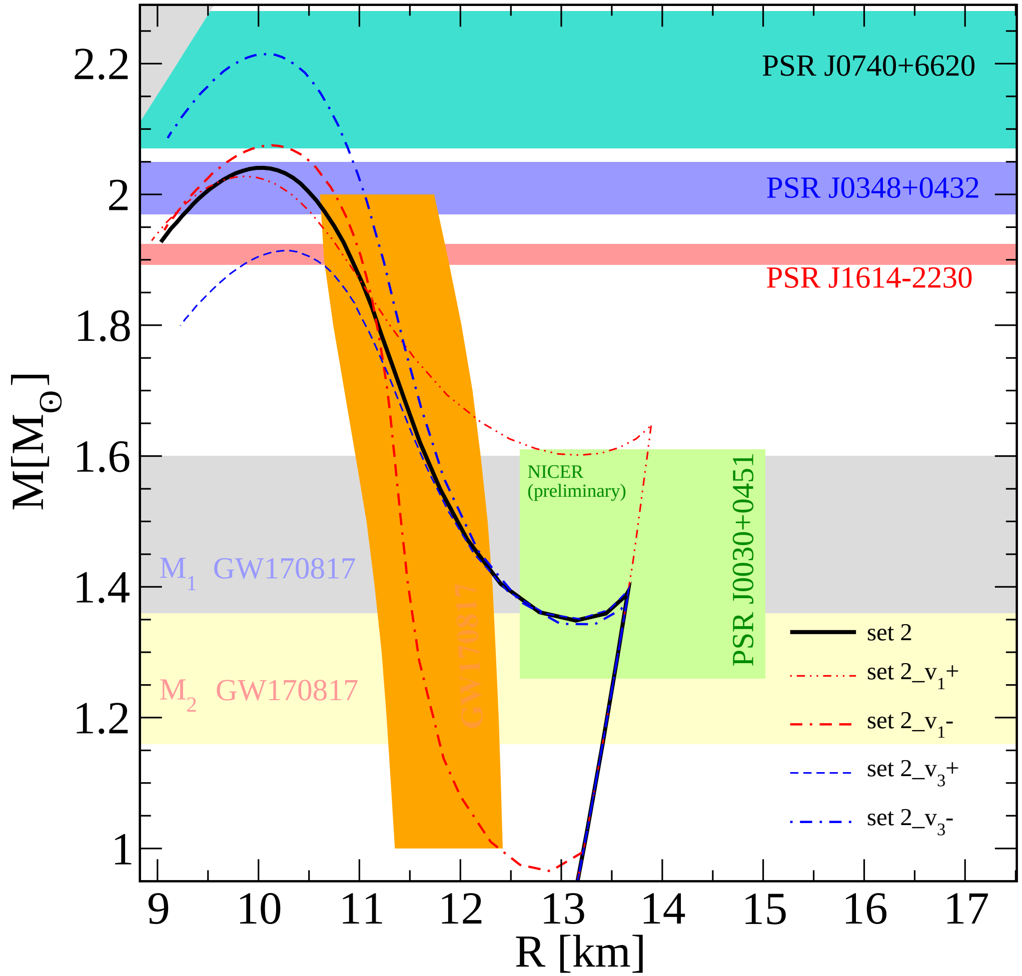

D. Alvarez-Castillo, D. Blaschke, G. Grunfeld, V. Pagura
Phys. Rev. D 99, 063010 (2019) - arXiv: 1805.04105

Nonlocal NJL

In this model we introduce a doubly interpolated non-local NJL quark matter EoS as follows:

$$P(\mu) = [f_<(\mu)P(\mu;\eta_<,B) + f_>(\mu)P(\mu;\eta_<,0)]f_\ll(\mu) + f_\gg(\mu)P(\mu;\eta_>,0)\ ,$$

where we have introduced two smooth switch-off functions, one that changes from one to zero at a lower chemical potential $\mu_<$ with a width $\Gamma_<$,

$$f_<(\mu) = \frac{1}{2}\left[1 - \tanh\left(\frac{\mu - \mu_<}{\Gamma_<}\right)\right],$$

and one that switches off at a higher chemical potential $\mu_\ll$ with a width $\Gamma_\ll$,

$$f_\ll(\mu) = \frac{1}{2}\left[1 - \tanh\left(\frac{\mu - \mu_\ll}{\Gamma_\ll}\right)\right],$$

whereby the corresponding switch-on functions are the complementary ones,

$$f_>(\mu) = 1 - f_<(\mu)\ ,\quad f_\gg(\mu) = 1 - f_\ll(\mu).$$

The input EoS differ in their η-values, we have taken for those values at low ($<$) and high ($>$) chemical potentials $\eta_<$ and $\eta_>$. Moreover, B represents a bag constant introduced to enforce confinement effects in the low chemical potential quark EoS.

D. Alvarez-Castillo, D. Blaschke, G. Grunfeld, V. Pagura
Phys. Rev. D 99, 063010 (2019) - arXiv: 1805.04105

GW170817 - Nonlocal NJL

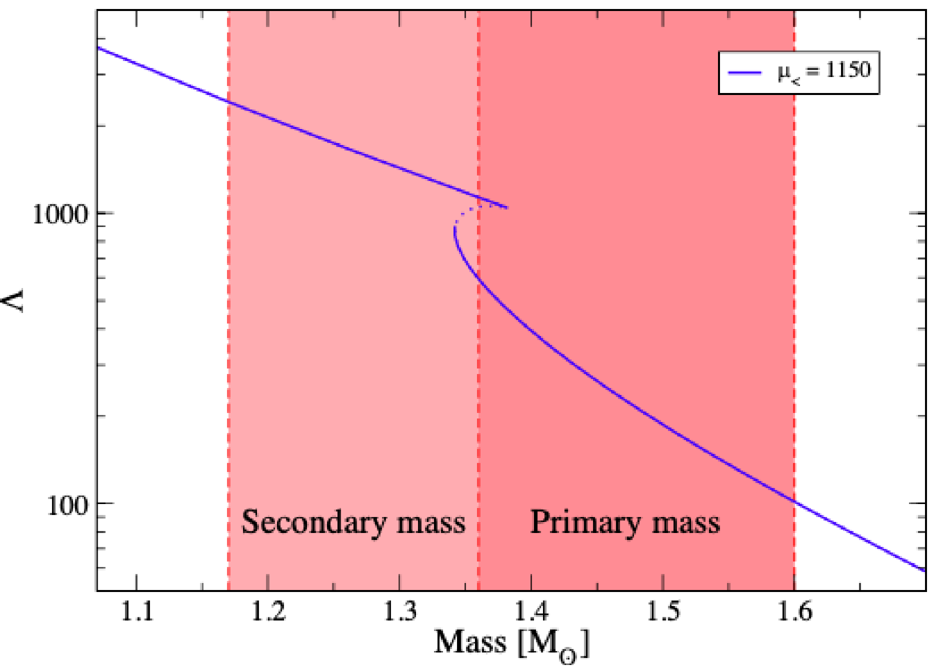

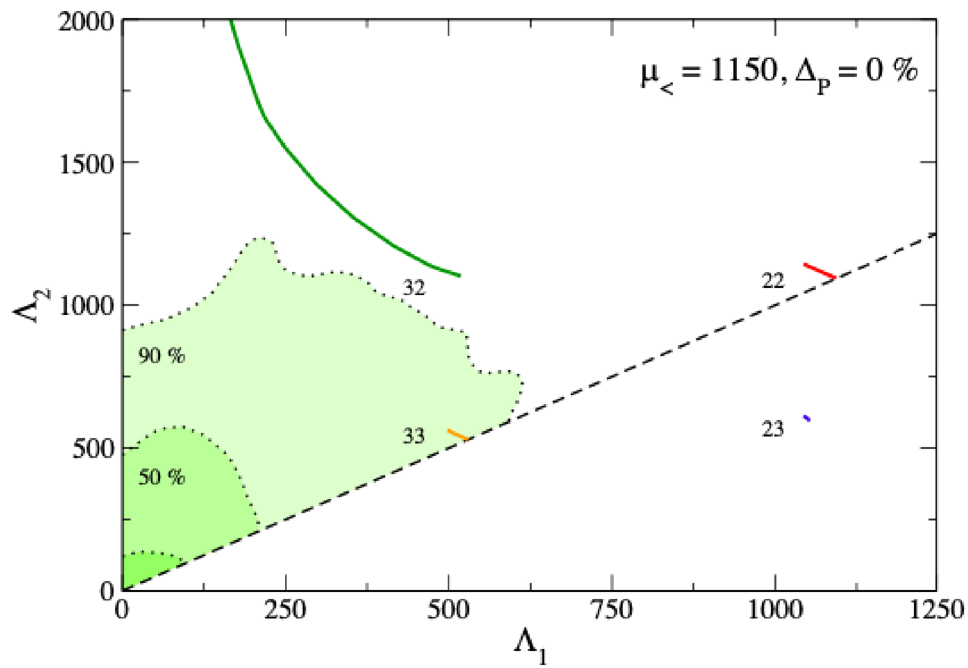

A. Ayriyan, D.Alvarez-Castillo, D. Blaschke and H. Grigorian,
in preparation

D. Alvarez-Castillo, D. Blaschke, G. Grunfeld, V. Pagura
Phys. Rev. D 99, 063010 (2019) - arXiv: 1805.04105

GW170817 - Nonlocal NJL

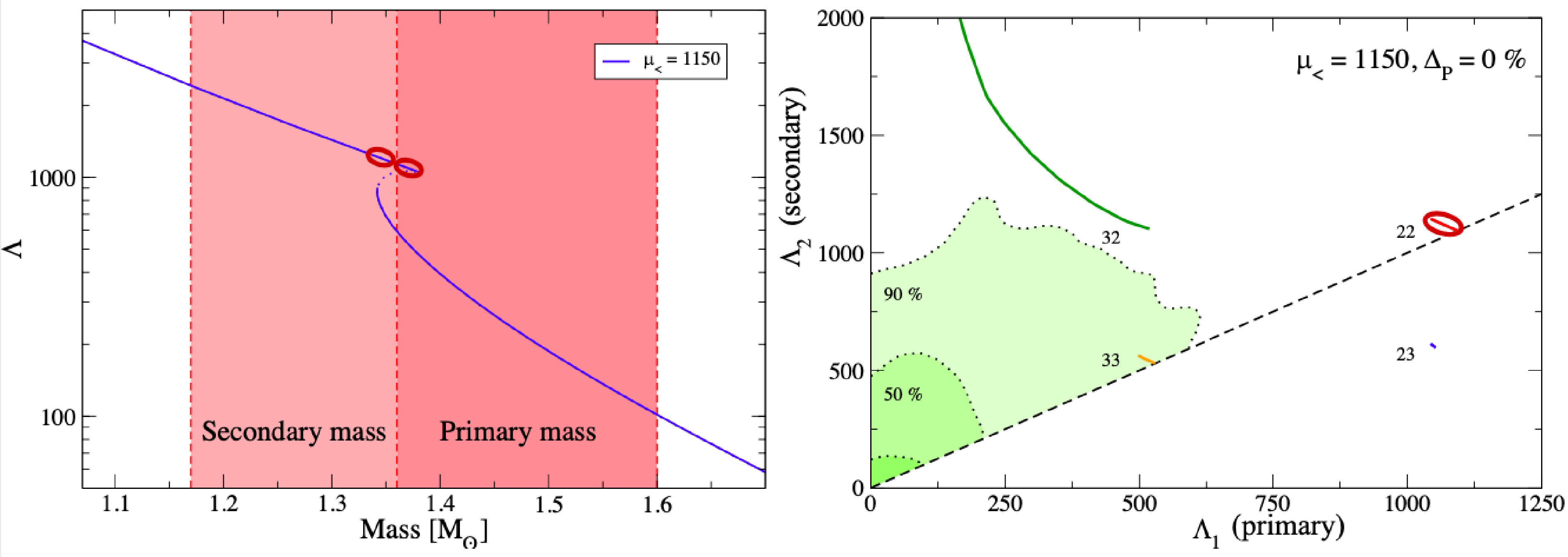

A. Ayriyan, D.Alvarez-Castillo, D. Blaschke and H. Grigorian,
in preparation

D. Alvarez-Castillo, D. Blaschke, G. Grunfeld, V. Pagura
Phys. Rev. D 99, 063010 (2019) - arXiv: 1805.04105

GW170817 - Nonlocal NJL

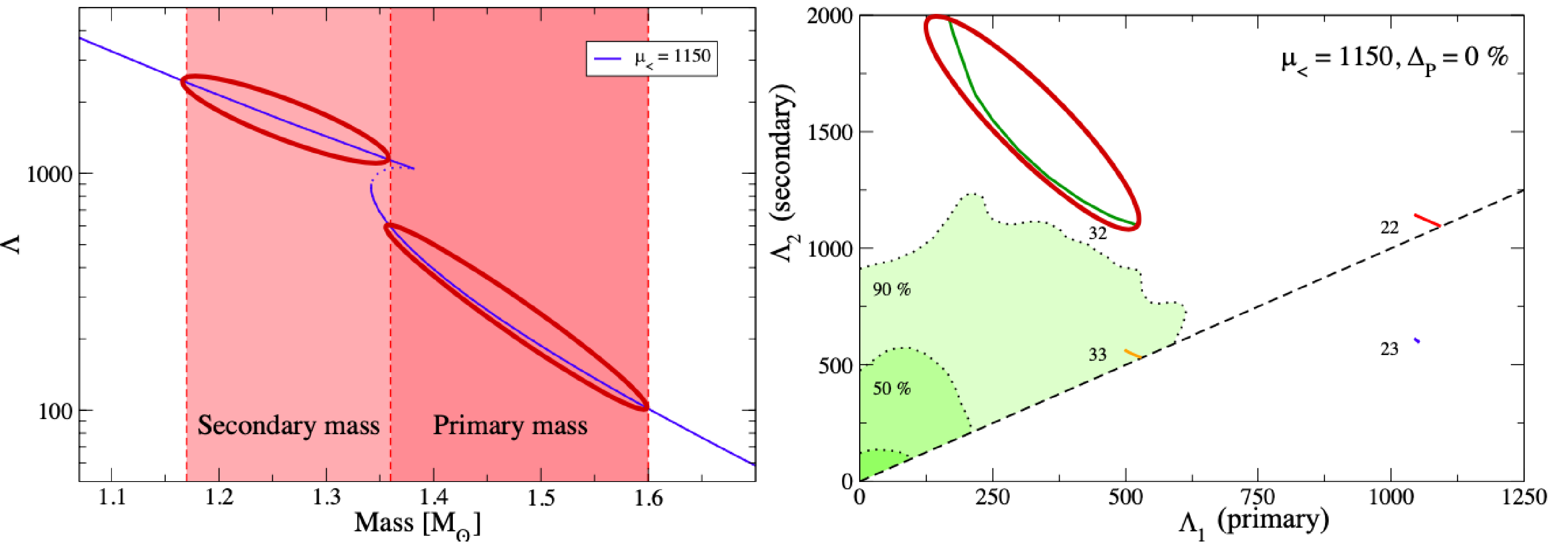

A. Ayriyan, D.Alvarez-Castillo, D. Blaschke and H. Grigorian,
in preparation

D. Alvarez-Castillo, D. Blaschke, G. Grunfeld, V. Pagura
Phys. Rev. D 99, 063010 (2019) - arXiv: 1805.04105

GW170817 - Nonlocal NJL

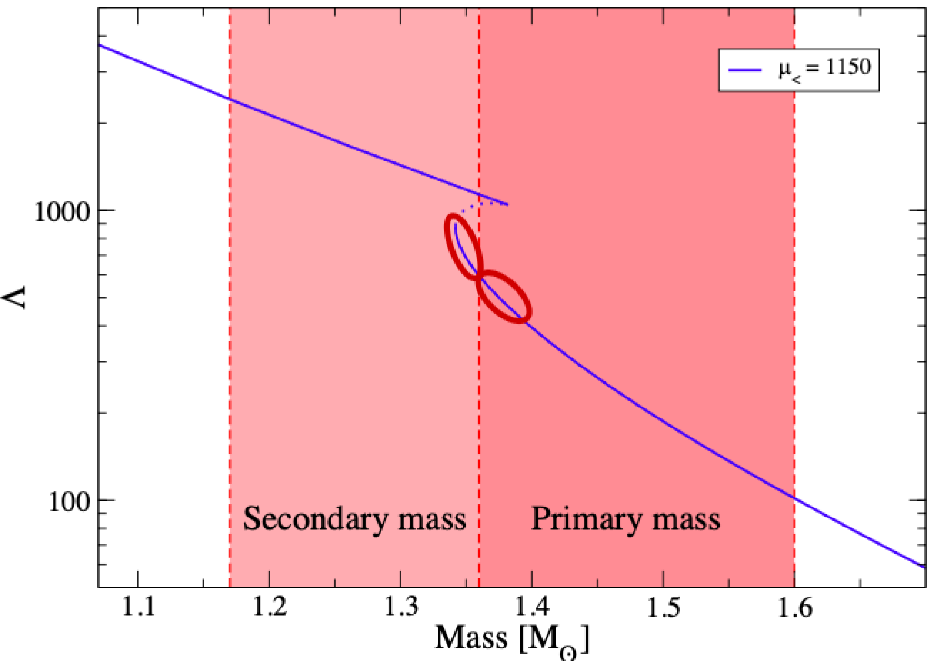

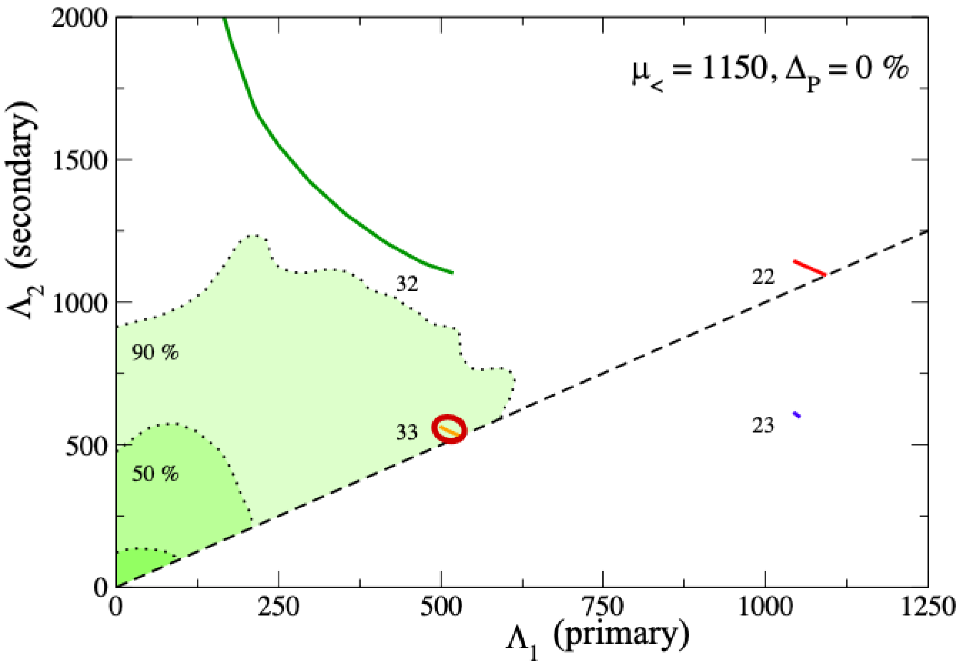

A. Ayriyan, D.Alvarez-Castillo, D. Blaschke and H. Grigorian,
in preparation

D. Alvarez-Castillo, D. Blaschke, G. Grunfeld, V. Pagura
Phys. Rev. D 99, 063010 (2019) - arXiv: 1805.04105

GW170817 - Nonlocal NJL

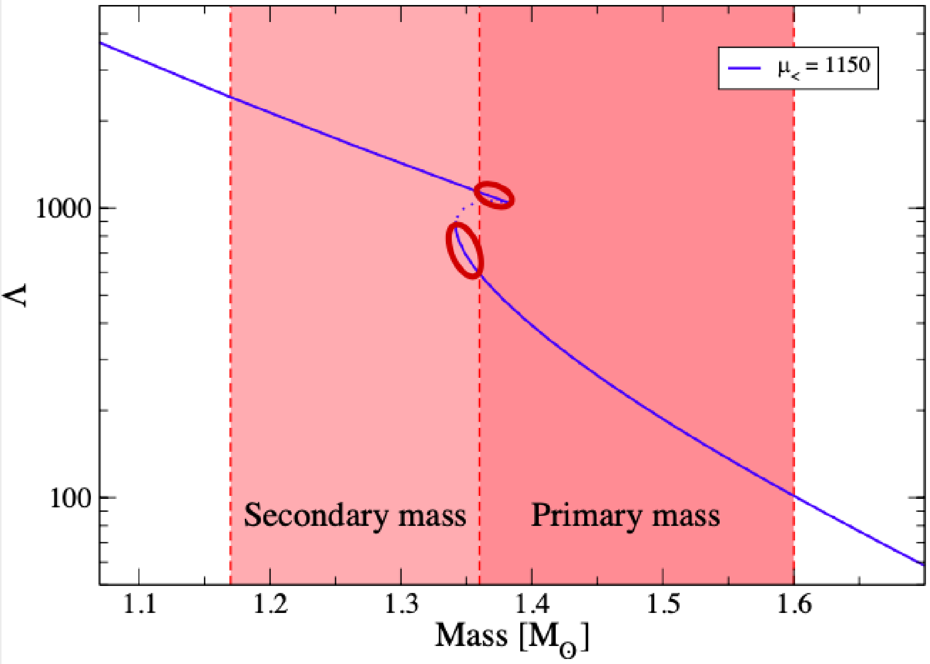

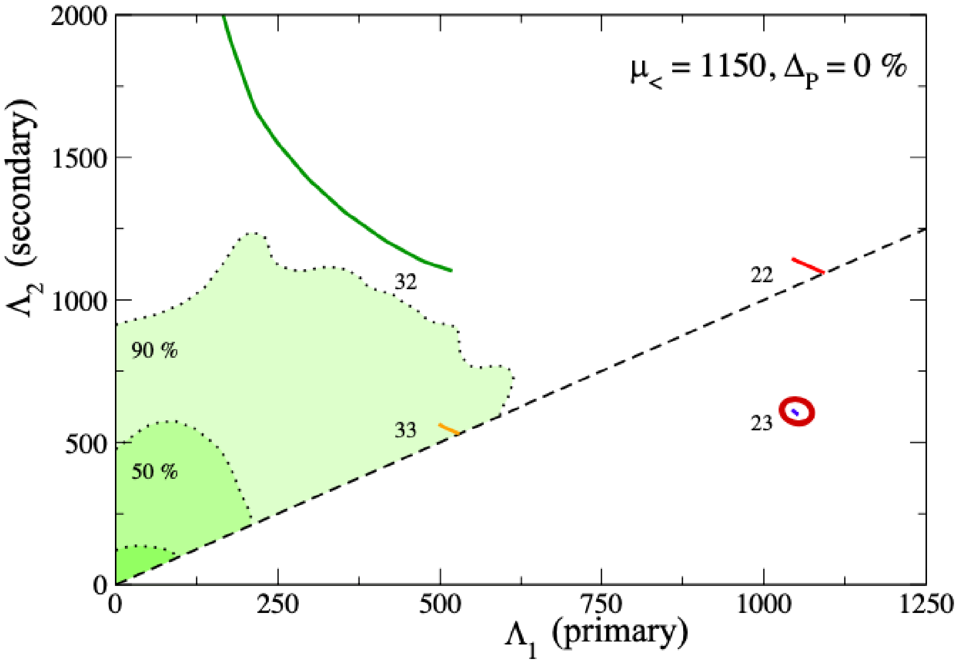

A. Ayriyan, D.Alvarez-Castillo, D. Blaschke and H. Grigorian,
in preparation

D. Alvarez-Castillo, D. Blaschke, G. Grunfeld, V. Pagura
Phys. Rev. D 99, 063010 (2019) - arXiv: 1805.04105

GW170817 - Nonlocal NJL

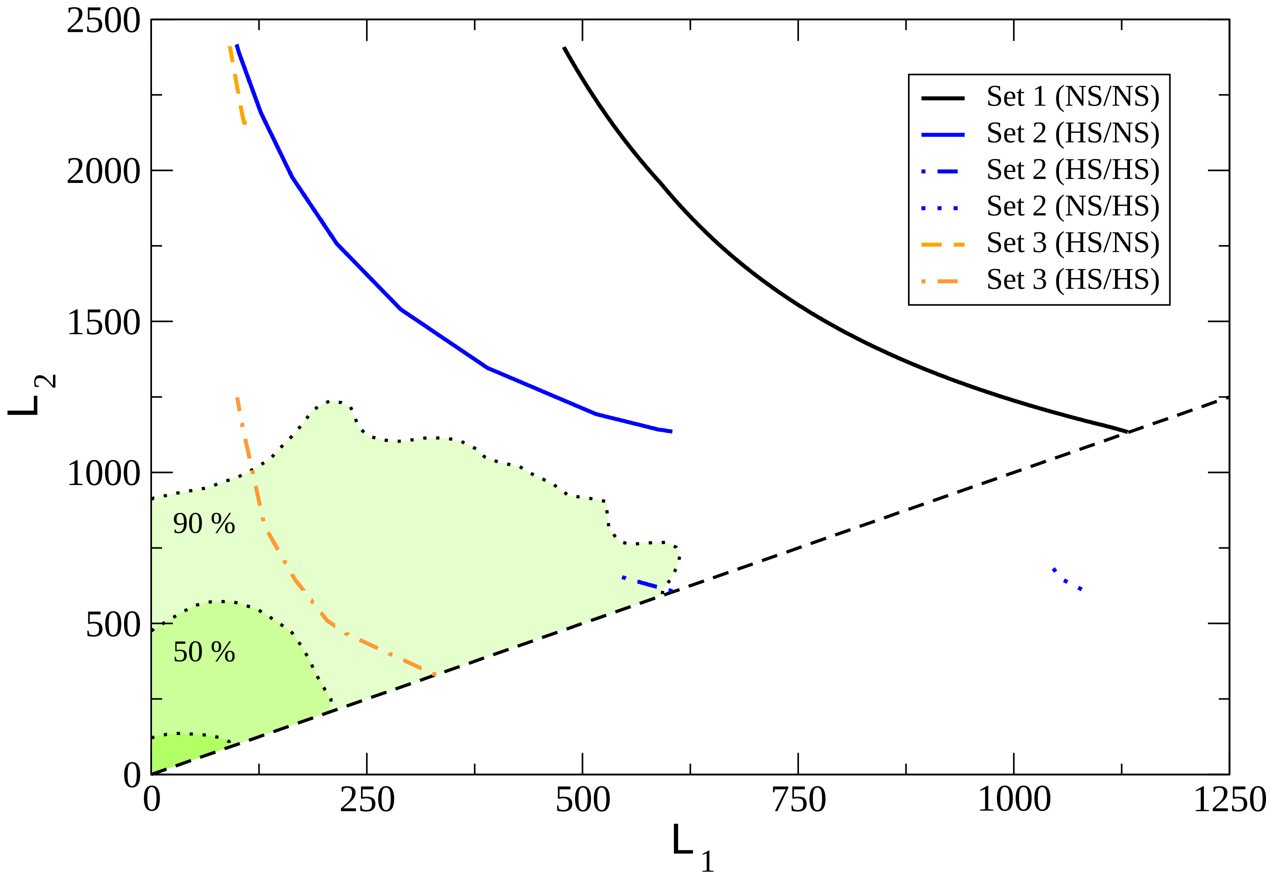

D. Alvarez-Castillo, D. Blaschke, G. Grunfeld, V. Pagura
Phys. Rev. D 99, 063010 (2019) - arXiv: 1805.04105

Gravitational Wave Signals
First Order Phase Transitions

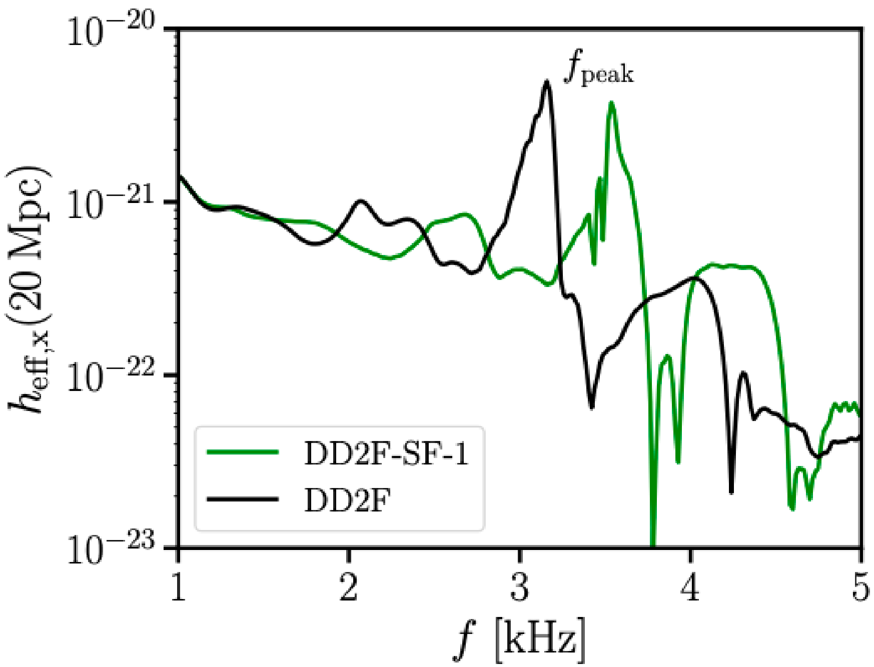

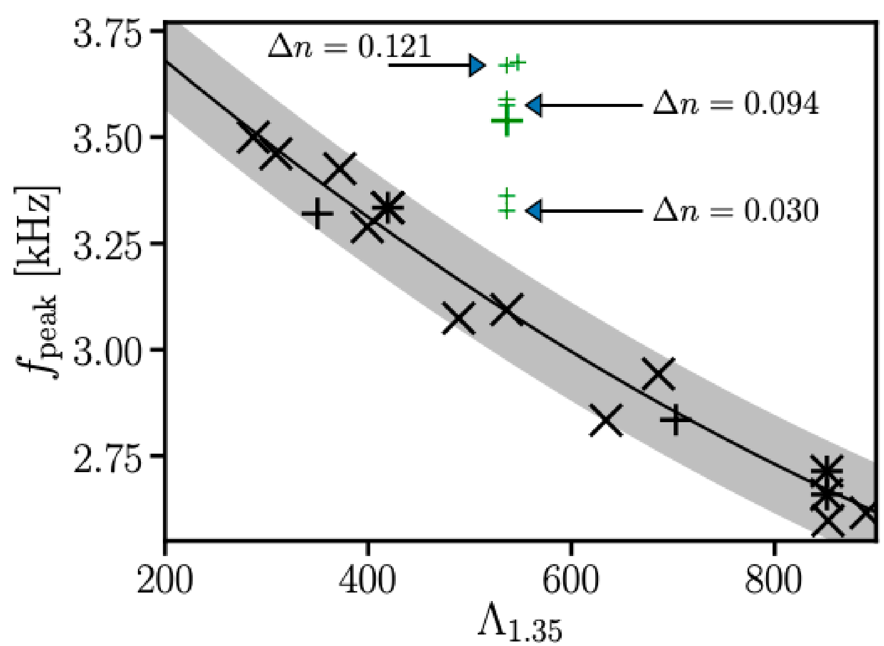

A. Bauswein et al. - arXiv: 1904.01306, PRL 122 (2019) 061102

Conclusions

- The equation of state at high densities must be effectively soft, either as a relatively soft hadronic one or a hybrid one with a strong phase transition.

- Future GW observations, NICER and SKA will soon result into stronger NS EoS constraints probing the mass twins hypothesis.

- Many possible astrophysical scenarios for mass twins could be confirmed implying a CEP in QCD.

Gracias